Westinghouse

Westinghouse Electric Company
Nuclear Power Plants
P.O. Box 355
Pittsburgh, Pennsylvania 15230-0355
USA

U.S. Nuclear Regulatory Commission
ATTENTION: Document Control Desk
Washington, D.C. 20555

Direct tel: 412-374-6206
Direct fax: 724-940-8505
e-mail: sisk1rb@westinghouse.com

Your ref: Docket Number 52-006
Our ref: DCP_NRC_002906

June 2, 2010

Subject: AP1000 Standard COL Technical Report Submittal of APP-GW-GLR-033, Revision 4 (TR54)

Westinghouse is submitting Revision 4 of AP1000 Standard Combined License Technical Report Number 54, "Spent Fuel Storage Rack Structure/Seismic Analysis." The purpose of Technical Report 54 (TR54) is to complete and document, on a generic basis, activities required for COL Information Item 9.1-3 in the AP1000 Design Control Document (DCD). Revision 4 incorporates changes made in response to additional NRC questions in May 2010, and changes resulting from the re-analysis of the spent fuel racks with the updated spectra. Pursuant to 10 CFR 50.30(b), APP-GW-GLR-033, Revision 4, "Spent Fuel Storage Rack Structure/Seismic Analysis," is submitted as Enclosure 1.

For historical reference, Revision 3 to TR54 incorporates finalized responses to additional NRC RAIs. The significant changes include the elimination of the fuel attenuation factor (RAI-SRP9.1.2-SEB1-05 Revision 1) and the reanalysis for modifications incorporated to obtain at least a 1.5 factor of safety against buckling in both the top and bottom of the cell walls (RAI-SRP9.1.2-SEB1-06 Revision 1 and -07 Revision 1). This revision also documents changes that were previously made to the spent fuel racks to hold a larger number of fuel assemblies. APP-GW-GLR-033, Revision 3 was submitted via letter DCP_NRC_002697, dated November 20, 2009. Revision 2 to Technical Report 54 incorporated changes made in response to NRC Requests for Additional Information (RAI), changes made in response to feedback received from the NRC during the May 2008 On-Site Technical Review, and changes resulting from the re-analysis of the spent fuel racks with the updated spectra as described in Technical Report 3, Revision 2 (TR03). The proposed changes included in Revision 2 of TR54 were changes to Revision 16 of the AP1000 DCD. Revision 2 was submitted via letter DCP/NRC2160, dated June 26, 2008. Revision 1 was submitted via DCP/NRC2130, dated May 2, 2008. Revision 0 was submitted via DCP/NRC1760, dated July 7, 2006.

This report is submitted in support of the AP1000 Design Certification Amendment Application (Docket No. 52-006). The information provided in this report is generic and is expected to apply to all Combined Operating License (COL) applicants referencing the AP1000 Design Certification and the AP1000 Design Certification Amendment Application.

D063
NRO

Questions or requests for additional information related to the content and preparation of this report should be directed to Westinghouse. Please send copies of such questions or requests to the prospective applicants for combined licenses referencing the AP1000 Design Certification. A representative for each applicant is included on the cc: list of this letter.

Very truly yours,

Robert Sisk, Manager
Licensing and Customer Interface
Regulatory Affairs and Strategy

/Enclosure

1. AP1000 Standard COL Technical Report Submittal of APP-GW-GLR-033, Revision 4 (TR54)

cc:	D. Jaffe	-	U.S. NRC	1E
	E. McKenna	-	U.S. NRC	1E
	P. Buckberg	-	U.S. NRC	1E
	T. Spink	-	TVA	1E
	P. Hastings	-	Duke Power	1E
	R. Kitchen	-	Progress Energy	1E
	A. Monroe	-	SCANA	1E
	P. Jacobs	-	Florida Power & Light	1E
	C. Pierce	-	Southern Company	1E
	E. Schmiech	-	Westinghouse	1E
	G. Zinke	-	NuStart/Entergy	1E
	R. Grumbir	-	NuStart	1E
	P. Loza	-	Westinghouse	1E

ENCLOSURE 1

APP-GW-GLR-033 (TR54)

Revision 4

"Spent Fuel Storage Rack Structure/Seismic Analysis."

AP1000 RECORD OF CHANGES

AP1000 DOCUMENT NO. APP-GW-GLR-033 REVISION 4

ALTERNATE DOC. NO. N/A

DESIGN AGENT ORGANIZATION Westinghouse Electric Co. LLC

TITLE Spent Fuel Storage Racks Structural/Seismic Analysis

CHANGE NUMBER	PARAGRAPH NUMBER	CHANGE DESCRIPTION AND REASON	ENGINEER APPROVAL/DATE
1	Entire Document	Made general administrative changes throughout entire document to make format and language consistent with APP-GW-GLR-026. Only major changes are discussed in this Record of Changes, but all changes throughout the document are shown with revision bars in the margin.	RJM/See EDMS
2	General	Updated document to reconcile the impact on the AP1000 Spent Fuel Storage Racks of the new seismic input contained in Reference 37.	RJM/See EDMS
3	2.2.1	Added a discussion about the new seismic input, and clarified the history of the existing input.	RJM/See EDMS
4	Table 2-6	Corrected materials properties and added Note 2.	RJM/See EDMS
5	Table 2-9	Updated and expanded table.	RJM/See EDMS
6	Table 2-12	Added evaluation of Cell Base Material Shear Stress, and updated results and corresponding safety factors. Note: the baseplate-to-cell weld size was increased, hence the increased safety factor.	RJM/See EDMS
7	Section 4	Added References 35 through 44.	RJM/See EDMS
8	Section 5	Deleted this section.	RJM/See EDMS

May 2010

AP1000 Standard Combined License Technical Report

Spent Fuel Storage Racks Structural/Seismic Analysis

Westinghouse Electric Company LLC
P.O. Box 355
Pittsburgh, PA 15230-0355

© 2010 Westinghouse Electric Company LLC
All Rights Reserved

TABLE OF CONTENTS

LIST OF TABLES 5

LIST OF FIGURES 6

1 INTRODUCTION 7
2 TECHNICAL BACKGROUND 8
2.1 DESIGN 8
2.1.1 AP1000 Spent Fuel Storage Racks Description 8
2.2 METHODOLOGY 10
2.2.1 Acceleration Time Histories 10
2.2.2 Modeling Methodology 11
2.2.3 Simulation and Solution Methodology 15
2.2.4 Conservatisms Inherent in Methodology 17
2.3 KINEMATIC AND STRESS ACCEPTANCE CRITERIA 17
2.3.1 Introduction 17
2.3.2 Kinematic Criteria 17
2.3.3 Stress Limit Criteria 17
2.3.4 Stress Limits for Various Conditions Per ASME Code 17
2.3.5 Dimensionless Stress Factors 20
2.4 ASSUMPTIONS 21
2.5 INPUT DATA 21
2.5.1 Rack Data 21
2.5.2 Structural Damping 21
2.5.3 Material Data 22
2.6 COMPUTER CODES 22
2.7 ANALYSES 22
2.7.1 Acceptance Criteria 22
2.7.2 Dynamic Simulations 22
2.8 RESULTS OF ANALYSES 22
2.8.1 Time History Simulation Results 22
2.8.2 Rack Structural Evaluation 24
2.8.3 Dead Load Evaluation 26
2.8.4 Local Stress Considerations 27
2.8.5 Hypothetical Fuel Assembly Drop Accidents 29
2.8.6 Stuck Fuel Assembly Evaluation 30
2.9 CONCLUSIONS 31
3 REGULATORY IMPACT 59
4 REFERENCES 60

LIST OF TABLES

Table 2-1 Region 1 Spent Fuel Storage Rack Storage Cell Description 32
Table 2-2 Region 2 Spent Fuel Storage Rack Storage Cell Description 32
Table 2-3 Defective Fuel Assembly Spent Fuel Storage Rack Storage Cell Description 33
Table 2-4 Simulations Listing 33
Table 2-5 Loading Combinations for AP1000 Spent Fuel Storage Racks 34
Table 2-6 Material Data 35
Table 2-7 AP1000 Spent Fuel Storage Rack Module and Fuel Data 36
Table 2-8 Computer Codes Used for Analysis 37
Table 2-9 Results Summary 38
Table 2-10 Deleted 38
Table 2-11 Maximum Pedestal and Cell Wall Stress Factors 39
Table 2-12 Baseplate-to-Cell Weld Maximum Stresses 40
Table 2-13 Deleted 40
Table 2-14 Baseplate-to-Pedestal Weld Maximum Stresses 40
Table 2-15 Pedestal Thread Shear Stress 40
Table 2-16 Cell-to-Cell Weld Maximum Stresses 40
Table 2-17 Deleted 40
Table 2-18 Degrees of Freedom for Single Rack Dynamic Model 41
Table 2-19 Results from Stuck Fuel Assembly Evaluation 41

LIST OF FIGURES

Figure 2-1 Spent Fuel Pool Storage Layout 42
Figure 2-2 Configuration of a Region 1 Storage Rack (Sheet 1 of 2) 43
Figure 2-2 Configuration of a Region 1 Storage Rack (Sheet 2 of 2) 44
Figure 2-3 Configuration of a Region 2 Storage Rack (Sheet 1 of 2) 45
Figure 2-3 Configuration of a Region 2 Storage Rack (Sheet 2 of 2) 46
Figure 2-4 Schematic Diagram of Dynamic Model for DYNARACK 47
Figure 2-5 Rack-to-Rack or Wall Impact Springs 48
Figure 2-6 Fuel-to-Rack Impact Springs at Level of Rattling Mass 49
Figure 2-7 Two-Dimensional View of Spring-Mass Simulation 50
Figure 2-8 Rack Degrees-of-Freedom for X-Y Plane Bending with Shear and Bending Spring 51
Figure 2-9 LS-DYNA Model of Dropped Fuel Assembly 52
Figure 2-10 LS-DYNA Model of Top and Bottom of AP1000 Region 1 Spent Fuel Rack 53
Figure 2-11 LS-DYNA Model of Top and Bottom of AP1000 Region 2 Spent Fuel Rack 54
Figure 2-12 Plastic Strain Results from Drop to Top of Region 2 Spent Fuel Rack 55
Figure 2-13 Maximum Rack Baseplate Deformation from Drop into an Empty Cell 56
Figure 2-14 Plastic Strain in Pool Liner from Drop over Rack Pedestal 57
Figure 2-15 Loading Pattern for Run Number 5 - Mixed Loading Case 58

1 INTRODUCTION

This report summarizes the structural/seismic analysis of the AP1000 Spent Fuel Storage Racks. Revision one specifically addresses Westinghouse responses to U.S. Nuclear Regulatory Commission (NRC) Requests for Additional Information (RAIs). Revision two specifically addresses three items: reanalysis of the spent fuel racks for the envelope of hard rock and soil conditions as documented in Reference 29; additional analysis requested by the NRC for mixed loading of the spent fuel racks and increased rack-to-rack gaps; and supplemental information added as a result of technical review meetings with the NRC during the period May 21 through May 22, 2008. Revision three incorporates finalized responses to additional NRC RAIs. Specifically, the significant changes include: the elimination of the fuel attenuation factor (as discussed in RAI-SRP9.1.2-SEB1-05) and the reanalysis to consider spent fuel rack design modifications that were incorporated to obtain at least a 1.5 factor of safety against buckling in both the top and bottom of the cell walls (as discussed in RAI-SRP9.1.2-SEB1-06 and RAI-SRP9.1.2-SEB1-07). Revision four reconciles the existing seismic analysis of the AP1000 Spent Fuel Storage Racks with the updated seismic input that is associated with the shield building enhancement and the correction of the SASSI model. Revision four also incorporates general administrative changes to address additional comments from the NRC and to clarify the report.

The AP1000 Spent Fuel Storage Racks are used to store fresh fuel assemblies prior to loading them in the reactor core and spent fuel assemblies after they have been discharged from the reactor core. The requirements for this analysis are identified in the AP1000 Design Control Document (DCD), subsection 9.1.2.2.1 (Reference 1). The completion of this analysis is identified as Combined Operating License (COL) Information Item 9.1-3 (Final Safety Evaluation Report [Reference 2] Action Item 9.1.6-3) in DCD subsection 9.1.6 to be completed by the Combined License applicant.

> COL Information Item 9.1-3: "Perform a confirmatory structural dynamic and stress analysis for the spent fuel rack, as described in subsection 9.1.2.2.1." This includes reconciliation of loads imposed by the spent fuel rack on the spent fuel pool structure described in subsection 3.8.4."

This COLA Technical Report addresses COL Information Item 9.1-3. The calculations "AP1000 Spent Fuel Storage Racks Structural/Seismic Analysis" (Reference 3) and "Analyses of AP1000 Fuel Storage Racks Subjected to Fuel Drop Accidents" (Reference 33) are available for U.S. NRC audit. ~~The reconciliation of loads imposed by the spent fuel racks on the spent pool structure described in DCD subsection 3.8.4 is provided in calculation, "Design of Spent Fuel Pit Floor in Module CA20," (Reference 27). The conclusion of that calculation is that the design of the fuel pool floor is adequate with respect to the loadings of completely filled spent fuel racks.~~

~~This report also documents changes that were previously made to the spent fuel racks to hold a larger number of fuel assemblies. The descriptions of the AP1000 Spent Fuel Storage Racks and analysis, as discussed in DCD subsection 9.1.2, "Spent Fuel Storage," and general arrangement, as discussed in DCD Section 1.2, "General Plant Description," of Reference 1, were previously updated to reflect the changes in the spent fuel racks with regard to their capacity to hold a greater number of fuel assemblies.~~

The reconciliation of loads imposed by the spent fuel racks on the spent pool structure described in DCD subsection 3.8.4 is provided in calculations, "Design of Spent Fuel Pit Floor in Module CA20,"

(Reference 27) and, "Auxiliary Building – CA20 Wall Basic Design Calculation," (Reference 35), with a reconciliation of the impact loads from the racks onto the spent fuel pool walls being addressed in Reference 34. The conclusion of these calculations is that the design of the spent fuel pool floor is adequate with respect to the loadings of completely filled spent fuel racks and that the walls and liner of the spent fuel pool are adequately designed to withstand the impact loads from the racks that may occur as a result of a seismic event, in combination with the additional loading conditions that the pool structure will be subjected to.

2 TECHNICAL BACKGROUND

This report considers the structural adequacy of the proposed AP1000 Spent Fuel Storage Racks under postulated loading conditions. Analyses and evaluations follow the U.S. NRC Standard Review Plan (SRP) 3.8.4, Revision 1 (Reference 6). Although the licensing basis for the AP1000 design invokes NRC SRP 3.8.4, Revision 1, an evaluation has been performed to confirm that the stress analysis of the spent fuel racks also satisfies the applicable provisions of NRC SRP 3.8.4, Revision 2 (Reference 31). The dynamic analyses use a time-history simulation code that has been used in numerous previous licensing efforts in the United States and abroad. This report provides a discussion of the method of analyses, modeling assumptions, key evaluations, and results obtained to establish the margins of safety. The objective of this report is to develop the loads on the AP1000 Spent Fuel Storage Racks and confirm that the loads do not pose a threat to the stored fuel assemblies.

2.1 DESIGN

2.1.1 AP1000 Spent Fuel Storage Racks Description

Figure 2-1 presents the storage layout of the AP1000 spent fuel pool. The total storage capacity is 889 locations. The AP1000 spent fuel pool contains three Region 1 rack modules and five Region 2 rack modules, one of which contains five Defective Fuel Assembly Storage Cells. ~~The Spent Fuel Pool Cooling System has the capability to cool a fully loaded spent fuel pool under the design basis conditions.~~

Note that Figure 2-1 shows the nominal rack-to-rack and rack-to-wall gaps. ~~Per DCD subsection 3.7.5.2, Combined License applicants will prepare site-specific procedures for activities following an earthquake. An activity of the procedures will be to address measurement of the post-seismic event gaps between the individual spent fuel racks and from the spent fuel racks to the spent fuel pool walls and to take appropriate corrective action if needed (such as repositioning the racks or analysis of the as-found condition).~~

There are three Region 1 modules, which are all 9x9 arrays of storage cells ~~(Reference 20). They are~~. The Region 1 spent fuel rack modules are designated Modules A1, A2, and A3. Note that the Region 1 modules are located along the west wall of the AP1000 spent fuel pool. Region 1 racks are designed to hold fresh and spent fuel assemblies in accordance with the limitations established by the results of the criticality analysis.

There are four Region 2 modules, which are 12x11 arrays of storage cells. The ~~12x11~~Region 2 spent fuel rack modules are designated Modules B1, B2, B3, and B4. These modules are located along the east wall of the AP1000 spent fuel pool. These racks are designed to hold fresh and spent fuel assemblies in accordance with the limitations established by the results of the criticality analysis.

There is a single 12x10 (-2) Region 2 module. It is designated Module C1. (Note that the term "12x10 (-2)" means a 12x10 array that is missing ~~seven~~a total of two storage cells. Seven Region 2 storage cells~~. The seven storage cells~~ are removed from the 12x10 array to provide space for the five Defective Fuel Assembly Storage Cells.) The five Defective Fuel Assembly Storage Cells ~~are designed to~~may hold fresh or spent fuel assemblies ~~that are defective~~ in accordance with the limitations established by the results of the criticality analysis.

2.1.1.1 Region 1 Storage Cell Description

Figure 2-2 presents the configuration of a Region 1 storage cell. The Region 1 storage cells are centered on a nominal pitch of 10.93 inches. Each storage cell consists of a stainless steel canister, which has a nominal inside dimension of 8.8 inches and is 0.090 inch thick. Metamic® neutron absorber panels are attached to the outside surfaces of the canister in all Region 1 storage cells except for the surfaces directly facing the west wall of the spent fuel pool. There are no neutron absorbers on the sides of the Region 1 racks facing the west walls because it is physically impossible to inadvertently place a fuel assembly in the space between the racks and the pool wall on that side. Each Metamic ~~poison~~neutron absorber panel is held in place and is centered on the width of the stainless steel canister by an outer stainless steel sheathing panel. There is a small void space (nominally 0.012 inch) between the sheathing and the Metamic panel. The dimensions of the Metamic ~~poison~~ neutron absorber panel are nominally 7.5 inches wide by 0.106 inch thick. The sheathing panels ~~on interior storage canisters~~ are 0.035 inch thick on the interior of the rack and 0.075 inch thick on the perimeter of the rack. For additional stability, 0.5 inch thick by 15 inch wide bumper bars are added around the entire perimeter of the Region 1 rack modules approximately 1.25 inches below the top of the racks.

Each Region 1 storage cell is approximately 199.5 inches long, and rests on top of a base~~-~~plate whose top is 5 inches above the spent fuel pool floor liner~~ floor~~. Note that each Metamic ~~poison~~ neutron absorber panel is 172 inches long and has a bottom elevation that is 6.23 inches above the top of the base~~-~~plate. The bottom elevation of the Metamic ~~poison~~ neutron absorber panel was positioned to be 2 inches lower than the bottom elevation of the active fuel. The Metamic ~~poison~~ neutron absorber material is a mixture of B_4C, nominally 31.0 weight-percent, and Al~~ with a nominal B_4C concentration equal to 31~~, nominally 69.~~0~~0 weight-percent~~, and uses natural boron isotopics (i.e., not enriched B^{10})~~. The Region 1 storage cell dimensions are summarized in Table 2-1.

2.1.1.2 Region 2 Storage Cell Description

Figure 2-3 presents the configuration of a Region 2 Storage Cell. The Region 2 storage cells are formed by welding open stainless steel canisters together at the corners. Therefore, the Region 2 storage cells are a combination of individual canister storage cells and "developed" storage cells. The "developed" storage cells result from the welding process. As an example, the welding of four canisters at the corners of each canister produces a single "developed" storage cell at the center of the four canisters. Each Region 2 ~~stainless steel canister~~ storage cell has ~~an~~ a nominal inside dimension of 8.8 inches, except the perimeter developed cells which have ~~an~~a nominal inside dimension of 8.89 inches, and is 0.090 inch thick. The center-to-center spacing between Region 2 storage cells is nominally 9.043 inches.

Metamic neutron absorber panels are attached to the outside surfaces of each stainless steel canister and on the filler panels used to create the perimeter developed cells, except for the surfaces directly facing the walls of the spent fuel pool. There are no neutron absorbers on the sides of the Region 2 racks facing the pool walls (except for one area on the C1 module) because it is physically impossible to inadvertently place a fuel assembly in the space between the racks and the pool walls. The exception is the C1 rack, where the Region 2 cells facing the west wall of the spent fuel pool have Metamic panels (this is because there is a small area to the south of the defective cells where the gap between the rack and the pool wall is large enough such that it is physically possible to inadvertently misplace a fuel assembly in this area; the accidental misplacement of a fuel assembly into this area is accounted for in the criticality analysis).

Each Metamic ~~poison~~neutron absorber panel is held in place and is centered on the width of the stainless steel canister by an outer stainless steel sheathing panel. There is a small void space (nominally 0.012 inch) between the sheathing and the Metamic panel. The dimensions of the Metamic ~~poison~~ neutron absorber panel are 7.5 inches wide by 0.106 inch thick. The sheathing panels ~~on interior storage canisters~~ are 0.035 inch thick on the interior of the rack and 0.075 inch thick on the perimeter of the rack. For additional stability, 0.5 inch thick by 15 inch wide bumper bars are added around the entire perimeter of the Region 2 rack modules approximately 0.25 inches below the top of the racks, and 0.105 inch thick local cell wall reinforcement ~~has~~ panels have been added directly above each Metamic ~~poison~~ neutron absorber panel and ~~extends~~they extend to 0.5 inches below the top of the cell walls.

Each Region 2 storage cell is approximately 199.5 inches long, and rests on top of a base~~-~~plate whose top is 5 inches above the spent fuel pool floor liner~~ floor~~. Note that each Metamic ~~poison~~ neutron absorber panel is 172 inches long and has a bottom elevation that is 6.23 inches above the top of the base~~-~~plate. The bottom elevation of the Metamic ~~poison~~neutron absorber panel was positioned to be 2 inches lower than the bottom elevation of the active fuel. The Metamic ~~poison~~ neutron absorber material is a mixture of B_4C, nominally 31.0 weight-percent, and Al~~ with a nominal B_4C concentration equal to 31~~, nominally 69.~~0~~0 weight-percent~~, and uses natural boron isotopics (i.e., not enriched B^{10})~~. The Region 2 storage cell dimensions are summarized in Table 2-2.

2.1.1.3 Defective Fuel Assembly Storage Cell

The Defective Fuel Assembly Storage Cells consist of ~~open~~ stainless canisters with ~~an~~ a nominal inside dimension of 10.25 inches and a thickness of 0.090 inch. The center-to-center spacing between the defective fuel assembly storage cells is 11.65 inches. Metamic panels are attached to the outside surfaces of each stainless steel canister except for the surfaces directly facing the west wall of the spent fuel pool. Each Metamic ~~poison~~ neutron absorber panel is held in place and is centered on the width of the stainless steel canister by an outer stainless steel sheathing panel. There is a small void space (nominally 0.012 inch) between the sheathing and the Metamic panel. The dimensions of the Metamic ~~poison~~ neutron absorber panel are 7.5 inches wide by 0.106 inch thick. The sheathing panels ~~on interior facing walls~~ are 0.035 inch thick on the interior ~~of the rack~~cells and 0.075 inch thick on the ~~perimeter of the rack~~exterior cells. For additional stability, 0.5 inch thick by 15 inch wide bumper bars are added around the perimeter of the Defective Fuel Assembly Storage Cells approximately 0.25 inches below the top of the cells.

Each Defective Fuel Assembly Storage Cell is approximately 199.5 inches long, and each rests on top of a base~~-~~plate whose top is 5 inches above the spent fuel pool floor liner~~ floor~~. Note that each Metamic ~~poison~~ neutron absorber panel is 172 inches long, and each has a bottom elevation that is 6.23 inches above the top of the base~~-~~plate. The bottom elevation of the Metamic ~~poison~~ neutron absorber panel was positioned to be 2 inches lower than the bottom elevation of the active fuel. The Metamic ~~poison~~neutron absorber material is a mixture of B_4C~~(~~, nominally 31.0 weight-percent~~)~~, and Al~~(~~, nominally 69.~~0~~0 weight~~-~~-percent~~)~~. The Defective Fuel Assembly ~~Storage Cell~~storage cell dimensions are summarized in Table 2-3.

2.2 METHODOLOGY

2.2.1 Acceleration Time Histories

The response of a freestanding rack module to seismic inputs is highly nonlinear, and it involves a complex combination of motions (sliding, rocking, twisting, and turning), resulting in impacts and frictional effects. Linear methods, such as modal analysis and response spectrum techniques, cannot accurately replicate the response of such a highly nonlinear structure to seismic excitation. An accurate simulation is obtained only by direct integration of the nonlinear equations of motion using actual pool ~~slab~~ floor acceleration time-histories as the forcing function. Therefore, the initial step in AP1000 Spent Fuel Storage Racks qualification is to develop synthetic time-histories for three orthogonal directions, which comply with the guidelines of the U.S. NRC Standard Review Plan 3.7.1, Revision 2 (Reference 8). In particular, the synthetic time-histories must meet the criteria of statistical independence, envelope the target design response spectra, and envelope the target Power Spectral Density function associated with the target response spectra.

The ~~ASB99~~ design basis AP1000 Nuclear Island Floor Response Spectra (FRS) were developed by Westinghouse in Reference 36 (which provides technical input for Reference 29), and these spectra envelope the hard rock and soil cases. ~~These~~The specific FRS ~~were~~for the AP1000 Spent Fuel Storage Racks was selected by Westinghouse from the data contained in Reference 36 and was transmitted to Holtec International in Reference 19. The synthetic time-histories for the ~~ASB99 Floor Response Spectra (FRS) were~~ "Spent Fuel" FRS (which is the name given to the specific FRS that was determined by Westinghouse to be applicable for the seismic analysis of the AP1000 Spent Fuel Storage Racks) were generated by Holtec International and form the basis of the seismic analysis performed in Reference 3. ~~The ASB99 FRS represent the enveloping response spectra for the Auxiliary and Shield Building (ASB) at Elevation 99 feet for a range of soil/rock condition. FRS of various soil/rock analyses were first enveloped for various locations of the ASB. All of the ASB locations at Elevation 99 feet were then grouped and enveloped to develop the ASB99 floor response spectra.~~ The ASB99 FRS contained in Reference 36 represent the standard grouping of enveloped response spectra for the Auxiliary and Shield Building (ASB) at Elevation 99 feet for a range of soil/rock conditions. The ASB locations nearest the four corners of the Spent Fuel Pool at Elevation 99 feet were grouped and enveloped to develop the "Spent Fuel" FRS. The floor of the Spent Fuel Pool is at a slightly lower elevation (Elevation 92'-8.5") but the dynamic response is essentially the same as at Elevation 99 feet.

The acceleration time histories for the ~~ASB99 FRS~~"Spent Fuel" FRS noted above are used as the input motion for the seismic analysis of the ~~spent fuel racks~~AP1000 Spent Fuel Storage Racks and form the design and licensing basis. The three orthogonal components are input and solved simultaneously together with a constant 1-g gravity acceleration. The generation of these acceleration time-histories is documented in Reference 38.

Updated seismic input for the AP1000 Spent Fuel Storage Racks, which incorporates the shield building design enhancements as well as the correction of the SASSI model, was made available in May 2010 via Reference 37 (which is based on the data contained in Reference 40, which provides technical input to Reference 41) and was transmitted to Holtec International in Reference 39. This new input has been evaluated and shown to result almost entirely in reduced loads on the Spent Fuel Storage Racks when compared to the current design and licensing basis seismic input. In all instances the maximum load that

resulted from the most severe case of all simulations decreased when using the seismic input based on Reference 37 compared to the seismic input based on Reference 36, as summarized in Table 2-9. However, for conservatism, the current seismic input as discussed in the preceding paragraphs (the input based on Reference 36) will remain the design and licensing basis for the AP1000 Spent Fuel Storage Racks.

2.2.2 Modeling Methodology

2.2.2.1 General Considerations

Once a set of input excitations is obtained, a dynamic representation is developed. Reliable assessment of the stress field and kinematic behavior of the rack modules calls for a conservative dynamic model incorporating all key attributes of the actual structure. This means that the dynamic model must have the ability to execute concurrent sliding, rocking, bending, twisting, and other motion forms compatible with the freestanding installation of the modules. Additionally, the model must possess the capability to effect momentum transfers that occur due to rattling of fuel assemblies inside storage cells and the capability to simulate lift-off and subsequent impact of support pedestals with the rack bearing pad or pool liner. The contribution of the water mass in the interstitial spaces around the rack modules and within the storage cells must be modeled in an accurate manner. The Coulomb friction coefficient at the pedestal~~-~~ to~~-~~ bearing pad and pool liner ~~interface~~interfaces may lie in a rather wide range~~ and a conservative value~~, depending on the design of ~~friction cannot be prescribed a priori~~ those interfaces, and the model must be able to reflect their effect. Finally, the analysis must consider that a rack module may be fully or partially loaded with fuel assemblies or may be entirely empty. The pattern of loading in a partially loaded rack may also have ~~innumerable~~ numerous combinations. In short, there are a large number of parameters with potential influence on the rack motion. A comprehensive structural evaluation must be able to incorporate all of these effects, in a finite number of analyses, without sacrificing conservatism.

The three-dimensional dynamic model of a single spent fuel rack was introduced by Holtec International in 1980 and has been used in many re-rack projects since that time. These re-rack projects include Turkey Point, St. Lucie, and Diablo Canyon. The details of this classical methodology are presented in Reference 10. The three-dimensional model of a typical ~~rack in the spent fuel pool~~AP1000 Spent Fuel Storage Rack handles the array of variables as follows:

- <u>Interface Coefficient of Friction</u>

  Coefficient of friction (COF) values are assigned at each interface, which reflect the realities of wetted stainless steel-to-stainless steel contact. The mean value of coefficient of friction is 0.5, and the limiting values are based on experimental data, which are bounded by the values 0.2 and 0.8 (Reference 21).

- <u>Impact Phenomena</u>

Compression-only spring elements, with gap capability, are used to provide for opening and closing of interfaces, such as the pedestal-to-bearing pad interface, the fuel assembly-to-cell wall interface, and the rack-to-rack and rack-to-pool wall potential contact locations.

- Fuel Loading Scenarios

The dynamic analyses performed for the AP1000 Spent Fuel Storage Racks assume that all fuel assemblies within the ~~rack~~racks rattle in unison throughout the seismic event, which ~~obviously~~ exaggerates the contribution of impact against the cell wall. In this analysis the fuel assemblies are considered to move perfectly in-phase (that is, the fuel assembly rattling attenuation factor equals one for all simulations).

- Fluid Coupling

Holtec International extended Fritz's classical two-body fluid coupling model (Reference 16) to multiple bodies and used it to perform a two-dimensional multi-rack analysis. Subsequently, laboratory experiments were conducted to validate the multi-rack fluid coupling theory. This technology is incorporated in the Whole Pool Multi-Rack (WPMR) analysis, which permits simultaneous simulation of all racks in the pool. In its simplest form, the so-called "fluid coupling effect" (References 11 and 16) can be explained by considering the proximate motion of two bodies under water. If one body (mass m_1) vibrates adjacent to a second body (mass m_2), and both bodies are submerged in frictionless fluid, then Newton's equations of motion for the two bodies are as follows:

$$(m_1 + M_{11}) A_1 + M_{12} A_2 = \text{applied forces on mass } m_1 + O(X_1^2)$$

$$M_{21} A_1 + (m_2 + M_{22}) A_2 = \text{applied forces on mass } m_2 + O(X_2^2)$$

A_1, A_2 denote absolute accelerations of masses m_1 and m_2, respectively, and the notation $O(X^2)$ denotes nonlinear terms. The fluid adds mass to the body (M_{11} to mass m_1), and an inertial force proportional to acceleration of the adjacent body (mass m_2). Thus, acceleration of one body affects the force field on another. This force field is a function of inter-body gap, reaching large values for small gaps. Lateral motion of a fuel assembly inside a storage location is subject to this effect. The fluid coupling, in general, is always present when a series of closely spaced bodies (fuel racks) undergo transient motion in a submerged environment (spent fuel pool). The fluid coupling effect encompasses interaction between every set of racks in the pool (that is, the motion of one rack produces fluid forces on all other racks and on the pool walls). Both near-field and far-field fluid coupling effects are included in the analysis. During the seismic event, all racks in the pool are subject to the input excitation simultaneously. The motion of each freestanding module is autonomous and independent of the others as long as they do not impact each other and no water is present in the pool. ~~As noted in References 11 and 16, the fluid forces can reach rather large values in closely spaced geometries.~~ It is, therefore, essential that the contribution of the fluid forces be included in a comprehensive manner. This is possible only if all racks in the pool are allowed to execute three-dimensional motion in the mathematical model. The fluid coupling effects between all freestanding racks must be included in the model to

properly account for the interaction of the hydrodynamic forces with the inertia and friction forces. The WPMR model simulates the three-dimensional motion of all modules simultaneously. The derivation of the fluid coupling matrix relies on the principle of continuity and Kelvin's recirculation theorem. The derivation of the fluid coupling matrix has been verified by an extensive set of shake table experiments (References 7 and 16).

2.2.2.2 Specific Modeling Details for a Single Rack

The "building block" for the WPMR analysis is a three-dimensional multi-degree of freedom model for each single spent fuel rack. For the WPMR dynamic analysis, each rack, plus contained rattling fuel, is modeled as a 22 Degree of Freedom (DOF) system. The rack cellular structure elasticity is modeled by a three-dimensional beam having 12 DOF (three translational and three rotational DOF at each end so that two-plane bending, tension/compression, and twisting of the rack are accommodated). An additional two horizontal DOF are ascribed to each of five rattling fuel masses, which are located at heights 0H, 0.25H, 0.5H, 0.75H, and H, where H is the height of a storage cell above the baseplate. While the horizontal motion of the rattling fuel mass is associated with five separate masses, the totality of the fuel mass is associated with the vertical motion and it is assumed that there is no fuel rattling in the vertical direction. In other words, the vertical displacement of the fuel is coupled with the vertical displacement of the rack (that is, degree of freedom "P3" in Figure 2-4) by lumping the entire stored fuel mass (in the vertical direction only) with the vertical rack mass at the baseplate level.

The beam model for the rack is assumed supported, at the base level, on four pedestals modeled with non-linear elements; these elements are properly located with respect to the centerline of the rack beam, and allow for arbitrary rocking and sliding motions. The horizontal rattling fuel masses transfer load to the spent fuel rack through compression-only gap spring elements, oriented to allow impacts of each of the five rattling fuel masses with the rack cell in either or both horizontal directions at any instant in time. Figure 2-4 illustrates the typical dynamic rack model with the degrees of freedom shown for both the AP1000 Spent Fuel Storage Racks and for the rattling fuel mass. Table 2-18 defines the nodal DOF for the dynamic model of a single rack as depicted in Figure 2-4. In order to simulate this behavior, the stored fuel mass is distributed among the five lumped mass nodes, for all racks, as follows:

	% of total stored fuel mass
• Top of rack (Node 2)	12.5%
• 3/4 height (Node 3)	25%
• 1/2 height (Node 4)	25%
• 1/4 height (Node 5)	25%
• Bottom of rack (Node 1)	12.5%

~~(See Figure 2-4.)~~

The stiffness of the pedestal springs that simulate rack pedestal to ~~the~~ spent fuel pool floor/liner compression-only contact is modeled using contact and friction elements at the locations ~~of~~ between the pedestals ~~between pedestal~~ and floor liner. Four contact springs (one at each corner location) and eight friction elements (two per pedestal) are included in each 22 DOF rack model.

Also shown in Figure 2-4 is a model detail of a typical support with a vertical compression-only gap element and two orthogonal elements modeling frictional behavior. These friction elements resist lateral loads, at each instant in time, up to a limiting value set by the current value of the normal force times the coefficient of friction. Figures 2-5 through 2-7 show schematic diagrams of the various (linear and non-linear) elements that are used in the dynamic model of a typical spent fuel rack. Specifically, Figure 2-5 shows the location of the compression-only gap elements that are used to simulate the potential for rack-to-rack or rack-to-wall contact at every instant in time. Figure 2-6 shows the four compression-only gap elements at each rattling mass location, which serve to simulate rack-to-fuel assembly impact in any orientation at each instant in time. Figure 2-7 shows a two-dimensional elevation schematic depicting the five fuel masses and their associated gap/impact elements~~,~~ as well as the typical pedestal friction and gap impact spring elements. This figure combines many of the features shown in Figures 2-5 and 2-6, and it provides an overall illustration of the dynamic model used for the AP1000 Spent Fuel Storage Racks.

Finally, Figure 2-8 provides a schematic diagram of the coordinates and the beam springs used to simulate the elastic bending behavior and shear deformation of the rack cellular structure in two-plane bending. Not shown are the linear springs modeling the extension, compression, and twisting behavior of the cellular structure.

Mass Matrix

In addition to the structural masses, the following hydrodynamic effects of the pool water are included in the total mass matrix:

- Rack-to-fuel hydrodynamic mass due to fluid motion inside each of the rack cells
- Hydrodynamic mass due to fluid movement around racks in the interstitial spaces between modules
- Hydrodynamic mass effects under the baseplate of each rack

Stiffness Matrix

The spring stiffnesses associated with the elastic elements that model the behavior of the assemblage of cells within a rack are based on the representation developed in Reference 11. Tension-compression behavior and twisting behavior are each modeled by a single spring with linear or angular extension involving the appropriate coordinates at each end of the rack beam model. For simulation of the beam bending stiffness, a model is used consistent with the techniques of the reference based on a bending spring and a shear spring for each plane of bending, which connects the degrees of freedom associated with beam bending at each end of the rack. Impact and friction behavior is included using the piecewise linear formulations similarly taken from ~~the~~ Reference 11.

~~The AP1000 Spent Fuel Storage Racks are subject to the ASB99 Floor Response Spectra for the AP1000 Spent Fuel Racks provided in Reference 19. The simulation runs, which are summarized in Table 2-4, are performed to bound possible coefficient of friction values to verify convergence, to determine impact on rack-fuel loading, to determine impact of rack-to-rack gaps and to measure the sensitivity to variations in the spring stiffnesses used to model the behavior of the rack.~~

~~Run numbers 1 through 3 in Table 2-4 are the base set of runs, which bound the possible coefficients of friction at the interface between the rack support pedestals and the bearing pads. All of the remaining runs, runs 4 through 9, are identical to run 1 with the following exceptions:~~

- ~~Run number 4 considers increased rack to rack gaps consistent with those identified on the outline drawing (Reference 9). The gaps are modified in order to demonstrate the variation in results due to installation tolerances.~~

- ~~Run number 5 considers mixed fuel loading conditions as shown in Figure 2-15. The shaded boxes in Figure 2-15 represent the loading fraction and location where the assemblies were loaded in each rack. Note, rack module B3 was modeled as empty for this run.~~

- ~~Run number 6 considers decreasing the impact spring rates and rack beam stiffnesses by 20%.~~

- ~~Run number 7 considers increasing the impact spring rates and rack beam stiffnesses by 20%.~~

  ~~The purpose of run numbers 6 and 7 is to measure the sensitivity of the dynamic results to variations in the stiffness properties.~~

- ~~Run number 8 considers a reduction in the integration time step by a factor of 4 in order to verify that the solution is converged.~~

- ~~Run number 9 considers the effects of the spent fuel racks being completely empty.~~

2.2.3 Simulation and Solution Methodology

The WPMR analysis process is the vehicle available for displacement and load analysis of each rack in the pool, and it also serves to establish the presence or absence of specific rack-to-rack or rack-to-wall impacts during a seismic event. Recognizing that the analytical work effort must deal with stress and displacement criteria, the sequence of model development and analysis steps that are undertaken for each simulation are summarized in the following:

a. Prepare three-dimensional dynamic models of the assemblage of all rack modules in the pool. Include all fluid coupling interactions and mechanical couplings appropriate ~~to~~ for performing an accurate non-linear simulation.

b. Perform non-linear WPMR dynamic analyses for the assemblage of racks in the pool. Archive results for post-processing ~~appropriate~~ displacement and load outputs from the dynamic model.

c. Perform stress analysis of high stress areas for rack dynamic runs. Demonstrate compliance with American Society for Mechanical Engineers (ASME) Code Section III, ~~subsection~~Subsection NF (Reference 12) limits on stress and displacement. The high stress areas are associated with the pedestal-to-baseplate connection. In addition, some local evaluations are performed for the bounding case to ensure that the fuel remains protected under all impact loads.

For the transient analyses performed in part b described above, a step-by-step solution in time, which uses a central difference algorithm, is used to obtain a solution. The WPMR simulation model serves as the foundation for the analyses performed herein. The solver computer algorithm, implemented in the Holtec Proprietary Code MR216 (a.k.a. DYNARACK), is given in Reference 11, and the documentation of MR216 is presented in Reference 13.

Using the 22-DOF structural model for every rack that comprises a WPMR simulation, equations of motion corresponding to each degree-of-freedom are obtained using Lagrange's formulation of the dynamic equations of motion (Reference 11). The system kinetic energy includes contributions from the structural masses defined by the 22-DOF model.

Results are archived at appropriate time intervals for permanent record and for subsequent post-processing for structural integrity evaluations as follows:

- All generalized nodal displacement coordinate values in order to later determine ~~the motion of the~~ the motion of the rack
- All load values for linear springs representing beam elasticity
- All load values for compression-only gap springs representing pedestals, rack-to-fuel impact, and rack-to-rack and rack-to-pool wall impacts
- All load values for friction springs at the pedestal/~~platform~~bearing pad interface

Simulation Descriptions

The AP1000 Spent Fuel Storage Racks are subject to the "Spent Fuel" Floor Response Spectra provided in Reference 19. The simulation runs, which are summarized in Table 2-4, are performed to bound possible coefficient of friction values, to verify convergence, to determine impact on rack fuel loading, to determine impact of rack-to-rack gaps, and to measure the sensitivity to variations in the spring stiffnesses used to model the behavior of the rack.

Run numbers 1 through 3 in Table 2-4 are the base set of runs, which bound the possible coefficients of friction at the interface between the rack support pedestals, bearing pads, and the pool liner. The base runs evaluate the racks in the fully loaded condition and consider the coefficient of friction as 0.8, 0.5, and 0.2, for Run numbers 1, 2, and 3, respectively. All of the remaining runs, Run numbers 4 through 9, are identical to Run number 1 with the following exceptions:

- Run number 4 considers increased rack to rack gaps consistent with those identified on the outline drawing (Reference 9). The gaps are modified in order to demonstrate the variation in results due to installation tolerances.
- Run number 5 considers mixed fuel loading conditions as shown in Figure 2-15. The shaded boxes in Figure 2-15 represent the loading fraction and location where the assemblies were loaded in each rack. Note, rack module B3 was modeled as empty for this run.

- Run number 6 considers decreasing the impact spring rates and rack beam stiffnesses by 20%.
- Run number 7 considers increasing the impact spring rates and rack beam stiffnesses by 20%.

  The purpose of Run numbers 6 and 7 is to measure the sensitivity of the dynamic results to variations in the stiffness properties.
- Run number 8 considers a reduction in the integration time step by a factor of 4 in order to verify that the solution is converged.
- Run number 9 considers the effects of the spent fuel racks being completely empty.

2.2.4 Conservatisms Inherent in Methodology

The following item is a built-in conservatism:

- All fuel rattling mass at each level is assumed to move as a unit thus maximizing impact force and rack response.

2.3 KINEMATIC AND STRESS ACCEPTANCE CRITERIA

2.3.1 Introduction

The AP1000 Spent Fuel Storage Racks are designed as seismic Category I. The U.S. NRC Standard Review Plan 3.8.4 (Reference 6) states that the ASME Code, Section III, Subsection NF (Reference 12), as applicable for Class 3 components, is an appropriate vehicle for design. ~~In addition to this, the~~The stress analysis of the spent fuel racks also satisfies all of the applicable provisions in NRC Regulatory Guide 1.124, Revision 1 (Reference 28) for components designed by the linear elastic analysis method. An additional assessment has been performed ~~to confirm~~which confirmed that the stress analysis of the spent fuel racks also satisfies the applicable provisions of NRC Regulatory Guide 1.124, Revision 2 (Reference 32). In the following sections, the ASME limits are set down~~ first, followed by any modifications by project specification, where applicable~~.

2.3.2 Kinematic Criteria

The AP1000 Spent Fuel Storage Racks should not exhibit rotations to cause the rack to overturn (that is, ensure that the rack does not slide off the bearing pads, or exhibit a rotation sufficient to bring the center of mass over the corner pedestal).

2.3.3 Stress Limit Criteria

For thoroughness, the Standard Review Plan (Reference 6) load combinations were used. Stress limits must not be exceeded under the required load combinations. The loading combinations shown in Table 2-5 are applicable for freestanding racks that are made of steel. (Note that there is no operating basis earthquake [OBE] event defined for the AP1000; therefore, loading conditions associated with an OBE event are not considered.)

2.3.4 Stress Limits for Various Conditions Per ASME Code

Stress limits for Normal Conditions are derived from the ASME Code, Section III, ~~subsection~~Subsection NF. Parameters and terminology are in accordance with the ASME Code. The AP1000 Spent Fuel Storage Racks are freestanding; thus, there is minimal or no restraint against free thermal expansion at the base of the rack. Moreover, thermal stresses are secondary, which strictly speaking, have no stipulated stress limits in Class 3 structures or components when acting in concert with seismic loadings. Thermal loads applied to the ~~rack~~racks are, therefore, not included in the stress combinations involving seismic loadings.

Material properties for ~~analysis~~the analyses and stress ~~evaluation~~evaluations are provided in Table 2-6.

2.3.4.1 Normal Conditions (Level A)

Normal conditions are as follows:

- Tension

  Allowable stress in tension on a net section is:

  $$F_t = 0.6\ S_y$$

  where S_y is the material yield strength at temperature. (F_t is equivalent to primary membrane stress.)

- Shear

  Allowable stress in shear on a net section is:

  $$F_v = 0.4\ S_y$$

- Compression

  Allowable stress in compression (F_a) on a net section of Austenitic material is:

  $$F_a = S_y(0.47 - kl/444r)$$

  where $kl/r < 120$ for all sections, and

  l = unsupported length of component.

  k = length coefficient which gives influence of boundary conditions, for example:
  k = 1 (simple support both ends)
  k = 2 (cantilever beam)
  k = 0.5 (clamped at both ends)

Note: Evaluations conservatively use k = 2 for all conditions.

r = radius of gyration of component = c/2.45 for a thin wall box section of mean side width c.

- Bending

Allowable bending stress (F_b) at the outermost fiber of a net section due to flexure about one plane of symmetry is:

$$F_b = 0.60\ S_y$$

- Combined Bending and Compression

Combined bending and compression on a net section satisfies:

$$f_a/F_a + C_{mx}f_{bx}/D_xF_{bx} + C_{my}f_{by}/D_yF_{by} < 1.0$$

where:

f_a	=	Direct compressive stress in the section
f_{bx}	=	Maximum bending stress for bending about x-axis
f_{by}	=	Maximum bending stress for bending about y-axis
C_{mx}	=	0.85
C_{my}	=	0.85
D_x	=	$1 - (f_a/F'_{ex})$
D_y	=	$1 - (f_a/F'_{ey})$
$F'_{ex,ey}$	=	$(\pi^2 E)/(2.15\ (kl/r)_{x,y}^2)$

and subscripts x and y reflect the particular bending plane.

- Combined Flexure and Axial Loads

Combined flexure and tension/compression on a net section satisfies:

$$(f_a/0.6\ S_y) + (f_{bx}/F_{bx}) + (f_{by}/F_{by}) < 1.0$$

- Welds

Allowable maximum shear stress (F_w) on the net section of a weld is:

$$F_w = 0.3\ S_u$$

where S_u is the material ultimate strength at temperature. For the area in contact with the base metal, the shear stress on the gross section is limited to $0.4S_y$.

2.3.4.2 Upset Conditions (Level B)

Although the ASME Code allows an increase in allowables above those appropriate for normal conditions, ~~any~~all evaluations performed herein conservatively use the normal condition allowables.

2.3.4.3 Faulted (Abnormal) Conditions (Level D)

Section F-1334 (ASME Section III, Appendix F [Reference 26]), states that limits for the Level D condition are the smaller of 2 or $1.167S_u/S_y$ times the corresponding limits for the Level A condition if $S_u > 1.2S_y$, or 1.4 if $S_u \leq 1.2S_y$ except for requirements specifically listed below. S_u and S_y are the ultimate strength and yield strength at the specified rack design temperature. Examination of material properties for 304L stainless demonstrates that 1.2 times the yield strength is less than the ultimate strength. Since 1.167 * (66,~~200~~100/21,300) = 3.~~63~~62, the multiplier of 2.0 controls. Note, the same conclusion is drawn if the properties of 304 stainless steel are considered; in this case 1.167 * (71,000/25,000) = 3.3.

Exceptions to the above general multiplier are the following:

- Stresses in shear in the base metal shall not exceed the lesser of $0.72S_y$ or $0.42S_u$. In the case of the austenitic stainless material used here, $0.72S_y$ governs.

- Axial compression loads shall be limited to 2/3 of the calculated buckling load.

- Combined Axial Compression and Bending – The equations for Level A conditions shall apply except that:

  F_a = 0.667 x Buckling Load/Gross Section Area,

  and $F_{ex,ey}$ may be increased by the factor 1.65.

- For welds, the Level D allowable maximum weld stress is not specified in Appendix F of the ASME Code. An appropriate limit for weld throat is conservatively set here as:

  $F_w = (0.3\ S_u)$ x factor

  where: factor = (Level D shear stress limit)/(Level A shear stress limit) = $0.72 \times S_y / 0.4 \times S_y = 1.8$

  therefore; $F_w = (0.3\ S_u) \times (1.8) = 0.54\ S_u$

2.3.5 Dimensionless Stress Factors

In accordance with the methodology of the ASME Code, Section NF, where both individual and combined stresses must remain below certain values, the stress results are presented in dimensionless form. Dimensionless stress factors are defined as the ratio of the actual developed stress to the specified limiting value. The limiting value of each stress factor is 1.0 based on an evaluation that uses the allowable strength appropriate to Level A or Level D loading as discussed above.

R_1 = Ratio of direct tensile or compressive stress on a net section to its allowable value (note pedestals only resist compression)

R_2 = Ratio of gross shear on a net section in the x-direction to its allowable value

R_3 = Ratio of maximum bending stress due to bending about the x-axis to its allowable value for the section

R_4 = Ratio of maximum bending stress due to bending about the y-axis to its allowable value for the section

R_5 = Combined flexure and compression factor (as defined in subsection 2.3.4.1)

R_6 = Combined flexure and tension (or compression) factor (as defined in subsection 2.3.4.1)

R_7 = Ratio of gross shear on a net section in the y-direction to its allowable value

At any location where stress factors are reported, the actual stress at that location may be recovered by multiplying the reported stress factor R by the allowable stress for that quantity. For example, if a reported Level A combined tension and two plane bending stress factor is $R_6 = 0.85$, and the allowable strength value is $0.6S_y$, then the actual combined stress at that location is Stress = $R_6 \times (0.6S_y) = 0.51S_y$.

2.4 ASSUMPTIONS

The following assumptions are used in the analysis:

- Fluid damping is neglected. This is a conservative assumption.
- ~~Modeling the~~The total effect of *n* individual fuel assemblies rattling inside the storage cells in a horizontal plane is modeled as one lumped mass at each of five levels in the fuel rack~~ is a conservative assumption~~. Thus, the effect of chaotic fuel mass movement is conservatively ignored.
- Fluid coupling forces are calculated based on the nominal fluid gaps prior to the seismic event. The fluid gaps are not updated according to the rack displacements.
- Rack Module C1 is comprised of 113 Region 2 cells plus 5 defective cells. This rack has been modeled as a 12 x 10 Region 2 rack. This is conservative because it assumes there are 120 storage locations, rather than 118, which increases the deadweight of the fully loaded rack and increases the rattling fuel mass during the SSE event.

2.5 INPUT DATA

2.5.1 Rack Data

Table 2-7 contains information regarding the AP1000 Spent Fuel Storage ~~Racks~~Rack Modules and ~~fuel data~~Fuel Data that are used in the analysis. Information is taken from the spent fuel rack drawings (Reference 9) unless noted otherwise.

2.5.2 Structural Damping

Associated with every stiffness element is a damping element with a coefficient consistent with 4% of critical linear viscous damping. This is consistent with the ~~ASB99 Design Basis~~"Spent Fuel" Floor Response Spectra set for the AP1000 Spent Fuel Storage Racks provided in Reference 19 and the Westinghouse AP1000 Seismic Design Criteria provided in Reference 22.

2.5.3 Material Data

The necessary material data ~~are~~ is shown in Table 2-6. This information is taken from ASME Code Section II, Part D (Reference 14). The values listed correspond to a temperature of 200°F, unless noted otherwise.

2.6 COMPUTER CODES

Computer codes used in this analysis are presented in Table 2-8.

2.7 ANALYSES

2.7.1 Acceptance Criteria

The dimensionless stress factors, discussed in subsection 2.3.5, must be less than 1.0. In addition:

- The compressive loads on the cell walls shall be shown to remain below two thirds of the critical buckling load (i.e., a minimum safety factor of 1.5 against buckling is maintained).
- Welds and base metal stresses must remain below the allowable stress limits corresponding to the material and load conditions, as discussed in greater detail in following sections.

2.7.2 Dynamic Simulations

As discussed earlier, nine simulations are performed. The simulations consider the ~~ASB99~~"Spent Fuel" Floor Response Spectra~~ and are required to satisfy the stress and kinematic criteria of Reference 6~~.

2.8 RESULTS OF ANALYSES

The following subsections contain the results obtained from the post-processor DYNAPOST (Reference 15) for the AP1000 Spent Fuel Storage Racks under the ~~ASB99~~"Spent Fuel" Floor Response Spectra.

2.8.1 Time History Simulation Results

Table 2-9 presents the results for major parameters of interest for the AP1000 Spent Fuel Storage Racks for each simulation. Run numbers are as listed in Table 2-4.

2.8.1.1 Rack Displacements

The post-processor results summarized in Table 2-~~10~~9 provide the maximum absolute displacements at the top and bottom corners (for any rack module in either the east-west or north-south direction~~a~~) relative to the pool ~~slab~~floor.

2.8.1.2 Pedestal Vertical Forces

Run number 7 provides the maximum vertical load on any pedestal. ~~This~~The results from this run (included in Table 2-9) may be used to assess the structural integrity of the pool ~~slab~~floor under the seismic event.

2.8.1.3 Pedestal Friction Forces

Run number 4 provides the maximum shear loads; the value is used as an input loading to evaluate the ~~female pedestal to~~ baseplate-to-pedestal weld stress (see Table 2-14).

2.8.1.4 Impact Loads

The impact loads~~—~~, such as fuel-to-cell wall, fuel-to-fuel, rack-to-rack, and rack-to-wall impacts~~—~~, are discussed below.

Fuel-to-Cell Wall and Fuel-to-Fuel Impact Loads

The maximum fuel-to-cell wall impact load, at any ~~level~~elevation in ~~the~~any rack, occurs during ~~run~~Run number 7.

For the five-lumped mass model (with 25% at the 1/4 points and 12.5% at the ends), the maximum g-load that the rack imparts on the fuel assembly can be computed as:

$$a = \frac{4F}{w} = 3.38 \cdot g$$

where:

a = maximum lateral acceleration in g's
F = maximum fuel-to-cell wall impact force (= 1,455 lbf)
w = weight of one fuel assembly (conservatively taken to be 1,720 lbs)

The maximum lateral acceleration is an order of magnitude less than the impact decelerations that fuel assemblies are typically qualified for in cask transport applications. Thus, the stored fuel assemblies inside the AP1000 Spent Fuel Storage Racks are capable of withstanding the maximum fuel-to-cell wall impact load.

The above results are based on the assumption that all fuel assemblies rattle in unison. In addition to this, out of phase fuel motion was evaluated to capture the worst case fuel-to-fuel impact load on a fuel assembly. When the fuel assemblies move out of phase it is possible for two adjacent fuel assemblies to accelerate towards one another and simultaneously impact the cell wall that separates them. The out of phase fuel-to-fuel impact evaluation shows that the maximum impact force on a single fuel spacer grid under SSE conditions is 2,447 lbf, which is less that the minimum allowable grid impact load of 3,837 lbf. This results in a factor of safety of approximately 1.57.

Rack-to-Rack and Rack-to-Wall Impacts

The top of a spent fuel rack may impact an adjacent rack or ~~the~~ a spent fuel pool ~~walls~~ wall as a result of ~~significant~~ rack rocking and/or sliding during a seismic event. The solver summary result files from Reference 13 in all of the simulations were manually scanned to determine the maximum impact on all sides of each rack. The maximum impact load from the pool walls onto the racks is summarized in Table 2-9. The bounding impact loads are as follows for each type of rack:

- Region I Rack: Maximum Impact Force = 328,600 lbf
- Region II Rack: Maximum Impact Force = 325,100 lbf

A conservative impact evaluation has been performed and documented in Reference 34 which concludes that these impact loads are acceptable on the spent fuel pool wall/liner, with no redesign required.

An LSDYNA model was developed to evaluate the structural integrity of the AP1000 Spent Fuel Storage ~~racks~~Racks against earthquake-induced impact buckling, which could buckle the cell walls, leading to unacceptable cell deformation, and to determine the allowable load before buckling. The allowable loads along with the corresponding safety factor against buckling are as follows for each type of rack:

- Region I Rack: Allowable Impact Load = 514,800 lbf; Safety Factor = 1.57
- Region II Rack: Allowable Impact Load = 570,200 lbf; Safety Factor = 1.75

The results show that the maximum compressive loads remain below two thirds the critical buckling load.

2.8.2 Rack Structural Evaluation

2.8.2.1 Rack Stress Factors

With time-history results available for pedestal normal and lateral interface forces, the limiting bending moment and shear force at the baseplate-to-pedestal interface may be computed as a function of time. In particular, maximum values for the previously defined stress factors can be determined for every pedestal in the AP1000 Spent Fuel Storage Racks. The maximum stress factor ~~for the AP1000 Spent Fuel Storage Racks~~ from each simulation is reported in ~~the result tables and~~ Table 2-9. Using this information, the structural integrity of the pedestal can be assessed. The net section maximum (in time) bending moments and shear forces can also be determined at the bottom of the cellular structure. Based on these, the maximum stress in the limiting rack cell (box) can be evaluated.

The summary of the maximum stress factors for the AP1000 Spent Fuel Storage Racks, for each of the simulations detailed in Table 2-4, is provided in Table 2-11. The ~~tables also report~~table reports the pedestal stress factor as well as the stress factors for the ~~AP1000 Spent Fuel Storage Racks~~ cellular cross section just above the baseplate. ~~These locations are~~ The cell area just above the baseplate is the most heavily loaded net section~~s~~ in the structure, so ~~that~~ satisfaction of the stress factor criteria at ~~these locations~~this location ensures that the overall structural criteria set forth in subsection 2.3.3 are met.

An adjustment factor accounting for the ASME Code slenderness ratio has been calculated. The adjustment factors are identified with * in ~~the~~ Table 2-11.

All stress factors, as defined in ~~Section~~section 2.3.5, are less than the ~~mandated~~required limit of 1.0 for all racks for the governing faulted condition examined. Therefore, the ~~rack is~~ AP1000 Spent Fuel Storage Racks are able to maintain ~~its~~their structural integrity under the worst loading conditions.

2.8.2.2 Weld Stresses

Weld locations in the AP1000 Spent Fuel Storage Racks subjected to significant seismic loading are at the bottom of the rack at the baseplate-to-cell connection, at the top of the pedestal support at the baseplate connection, and at the cell-to-cell connections. Bounding values of resultant loads are used to qualify the connections.

a. <u>Baseplate-to-Rack Cell Welds</u>

Reference 12 (ASME Code Section III, ~~subsection~~Subsection NF) permits, for Level A or B conditions, an allowable weld stress $\tau = .3\ S_u$. Conservatively assuming that the weld strength is the same as the lower base metal ultimate strength, the allowable stress is given by $\tau = .3 * (66,\cancel{200}100) = 19,\cancel{860}830$ psi. As stated in subsection 2.3.4.3, the allowable for Level D is 0.54 S_u, giving an allowable of 35,~~748~~694 psi.

Weld stresses are determined through the use of a simple conversion (ratio) factor (based on area ratios) applied to the corresponding stress factor in the adjacent rack material. This conversion factor is developed from the differences in base material thickness and length versus weld throat dimension and length:

$$\frac{0.090*(8.8+0.090)}{0.0781*0.7071*7.0}=2.069$$

where:

0.090 ~~=~~ = the cell wall thickness
8.8 + 0.090 ~~=~~ = the mean box dimension
0.~~0625~~0781*0.7071 = the box-baseplate fillet weld throat size
7.0 = = the length of the weld

The highest predicted cell-to-baseplate weld stress is calculated based on the highest R6 value for the rack cell region tension stress factor and R2 and R7 values for the rack cell region shear stress factors (see subsection 2.3.5 for definition of these factors). These cell wall stress factors are converted into weld stress values as follows:

$\{[R6 * (1.2)]^2 + [R2 * (0.72)]^2 + [R7 * (0.72)]^2\}^{1/2} * S_y * \text{Ratio} =$

$\{[0.434 * (1.2)]^2 + [0.070 * (0.72)]^2 + [0.067 * (0.72)]^{21/2} * (21{,}300) * 2.$~~586 = 28,943~~069 = 23,157 psi

The above calculations are conservative because the maximum stress factors used ~~above~~ do not all occur at the same time instant.

Table 2-12 shows that the maximum baseplate-to-rack cell weld ~~stresses~~stress and the corresponding cell base metal shear stress are acceptable and have safety factors greater than 1.

b. Baseplate-to-Pedestal Welds

The finite element code ANSYS is used to resolve tension and compression stresses in the baseplate-to-pedestal weld due to the combined effects of a vertical compressive load in the pedestal and a bending moment caused by pedestal friction. The compression interface between the baseplate and the pedestal is modeled using contact elements. The perimeter nodes on the pedestal are connected to the baseplate by spring elements in order to simulate tension in the weld. The maximum instantaneous friction force on a single pedestal from the rack seismic analysis is conservatively applied to the finite element model in the horizontal x- and y-directions simultaneously, along with the concurrent vertical load, at the appropriate offset location. The perimeter nodes on the pedestal are restrained to move only in the vertical direction so that the spring elements only resist bending. The limiting ANSYS results are combined with the maximum horizontal shear loads to obtain the maximum weld stress, which occurs at the corner of the pedestal where the tensile stress in the weld due to bending is at its maximum. Table 2-14 summarizes the result, showing a safety factor greater than 1.

c. Cell-to-Cell Welds

Cell-to-cell connections are by a series of connecting welds along the cell height. Stresses in storage cell-to-cell welds develop due to fuel assembly impacts with the cell wall. These weld stresses are conservatively calculated by assuming that fuel assemblies in adjacent cells are moving out of phase with one another so that impact loads in two adjacent cells are in opposite directions; this tends to separate the two cells from each other at the weld. ~~Cell~~The cell-to-cell weld calculations are based on the maximum stress factor from all runs. Both the weld stress and the cell base metal shear stress results are reported in Table 2-16, and show safety factors greater than 1.

2.8.2.3 Pedestal Thread Shear Stress

Table 2-15 provides the limiting pedestal thread ~~stresses~~ shear stress under faulted conditions. The maximum average shear stress in the engagement region is ~~17,501 psi~~calculated based on the vertical load, with the maximum occurring in Run number 7. This computed stress is applicable to both the male and female pedestal threads.

The allowable shear stress for Level D conditions is the lesser of: $0.72\ S_y = 19{,}224$ psi or $0.42\ S_u = 30{,}660$ psi (based on S_y and S_u for SA240-304 at 150°F). Therefore, the former criterion controls ~~and the limiting~~the allowable pedestal thread shear stress. The result ~~are~~is detailed in Table 2-15.

2.8.3 Dead Load Evaluation

The dead load condition is not a governing condition for ~~spent fuel racks~~the AP1000 Spent Fuel Storage Racks since the general level of loading is far less than the safe shutdown earthquake (SSE) load condition. ~~The maximum pedestal load~~To illustrate this, it is shown below that the maximum pedestal load, which occurs when a Region 2 rack is fully loaded, is relatively low~~,~~ and that further stress evaluations are unnecessary.

Description	Level A Maximum Pedestal Load (lbf)
Dry Weight of 12x11 Rack	24,600
Dry Weight of 132 Intact Fuel Assemblies	257,928
Total Dry Weight	282,528
Load per Pedestal	70,632

This load will induce low stress levels in the neighborhood of the pedestal, compared with the load levels that exist under the SSE load condition (that is, on the order of 404,000 lb ~~for this~~per rack~~). Therefore, there~~ pedestal). There are no primary shear loads on the pedestal, and since ~~the~~these Level A loads are ~~approximately~~well less than 20% of the Level D loads, while the Level A limits ~~exceed~~are greater than 50% of the Level D limits, the SSE load condition bounds the dead load condition and no further evaluation is ~~performed~~necessary for dead load only.

2.8.4 Local Stress Considerations

This subsection presents evaluations for the possibility of cell wall buckling and the secondary stresses produced by temperature effects.

2.8.4.1 Cell Wall Buckling Evaluation

An ANSYS analysis was performed to evaluate the buckling capacity of the AP1000 Spent Fuel Storage Rack cells at the base of the racks. The cell wall acts alone in compression for a length of about 6.23 inches up to the point where the neutron absorber sheathing is attached. Above this level the sheathing provides additional strength against buckling; therefore, the analysis focuses on the lower 6.23 inches of the cell wall.

The analysis only evaluates a Region 2 storage cell. A separate analysis of a Region 1 storage cell is not necessary because the Region 1 racks are inherently stronger due to each cell being constructed from a four-sided tube (rather than using filler panels or corner angles like the Region 2 cells) and because the maximum R6 stress factor for the Region 1 racks is less than the maximum R6 stress factor for the Region 2 racks.

~~A compressive force equivalent to 9,500 psi is applied to the ANSYS finite element model. It is conservative to use this value since the~~The maximum compressive stress ~~in the cells~~ under seismic loading is:

σ = (1.2) (21,300) (R6, which is taken to be 0.347) = 8,869 psi

The adjusted R6 value used for this calculation takes credit for an inherent modeling conservatism related to the DYNARACK post-processing method, and incorporates a weight ratio adjustment factor to appropriately reduce the axial force portion of the R6 calculation to a more realistic value for this application.

~~The above calculation is based on the maximum R6 stress factor after adjusting the net vertical force on the gross cell cross-section. The reason that the adjustment is made is to correct an over conservatism for this application related to the method for post-processing the DNYARACK results.~~

When the time history results from DYNARACK are post-processed (using the computer code DYNAPOST) to determine the maximum stress factors for each rack, the net vertical force is conservatively computed by summing the vertical forces on all 4 rack support pedestals at a given time instant. The vertical forces on the rack support pedestals reflect the amplified weight of the rack plus the stored fuel assemblies during the earthquake. Since the stored fuel assemblies are supported from below by the rack baseplate, and they are not physically connected to the cell walls, the actual compressive load on the rack cell structure is significantly less than the value determined by DYNAPOST. Therefore it is appropriate to use a modified R6 value for this application.

For conservatism, a compressive force equivalent to 9,500 psi is applied to the ANSYS finite element model. This force is then increased by a factor of 1.5 to ensure that the acceptance criteria in section 2.7.1 are met.

The ANSYS analysis demonstrates that the AP1000 Spent Fuel Storage Rack cells remain in a stable configuration under 1.5 times the conservative compressive stress discussed above that results from the maximum seismic load without any gross yielding of the storage cell wall, which satisfies the ASME Code requirements for Level D conditions.

2.8.4.2 Thermal Stress Evaluation of Isolated Hot Cell

The temperature gradients across the rack structure caused by differential heating effects between one or more filled cells and one or more adjacent empty cells are considered. The worst thermal stress field in a fuel rack is obtained when an isolated storage location has a fuel assembly generating heat at maximum postulated rate and the surrounding storage locations contain no fuel. This secondary stress condition is evaluated alone and not combined with primary stresses from other load conditions.

A thermal gradient between cells will develop when an isolated storage location contains a fuel assembly emitting ~~maximum postulated~~ heat, while the surrounding locations are empty. A conservative estimate of the weld stresses along the length of an isolated hot cell is obtained by considering a beam strip uniformly heated by 50°F, and restrained from growth along one long edge. The 50°F temperature rise envelops the difference between the maximum local spent fuel pool water temperature (174°F) inside a storage cell and the bulk pool temperature (140°F) based on the thermal-hydraulic analysis of the spent fuel pool (Reference 44). The cell wall configuration considered here is shown in the figure below.

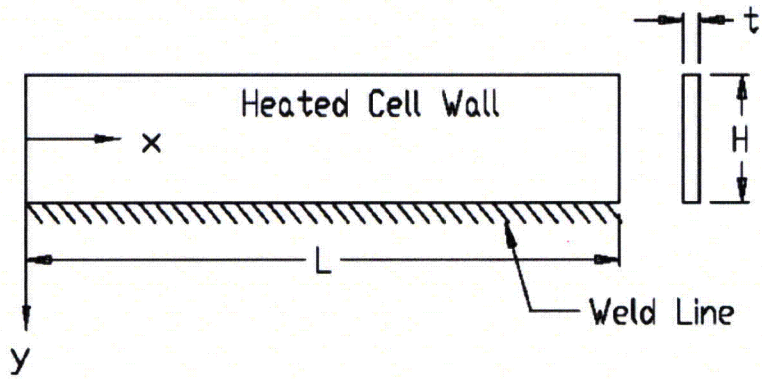

The strip is subjected to the following boundary conditions:

- Displacement U_x (x,y) = 0 at x = 0 and at y = H/2 for all x
- Average force N_x (x) = 0 at x = L

Using shear beam theory and subjecting the strip to a uniform temperature rise ΔT = 50°F, we can calculate an estimate of the maximum value of the average shear stress in the strip. The final shear stress result for the strip is found to be

$$\tau_{max} = \frac{E\alpha\Delta T}{0.931} \qquad \text{(maximum at x = L)}$$

where E = 27.6 x 10^6 psi, α = 9.5 x 10^{-6} in/in °F and ΔT = 50°F.

Therefore, we obtain an estimate of maximum weld shear stress in an isolated hot cell, due to thermal gradient, as

$$\tau_{max} = 14{,}082 \text{ psi}$$

Since this is a secondary thermal stress, the allowable shear stress criteria for this faulted ~~conditions~~condition is 27,762 psi (0.42*S_u~~=27,804 psi) is used to indicate that this maximum shear is acceptable~~). Therefore, there is a safety factor = 27,~~804~~762 / 14,082 = 1.97 against cell wall shear failure due to secondary thermal stresses from cell wall growth under the worst case hot cell conditions.

2.8.5 Hypothetical Fuel Assembly Drop Accidents

Three fuel assembly drop accident analyses have been performed for Region 1 and Region 2 spent fuel racks in accordance with subsection 9.1.2.2.1 C of Reference 1, and are documented in Reference 33. The objective of the analyses was to assess the extent of permanent damage to the rack and to evaluate the structural integrity of the spent fuel pool liner:

1) A drop of a fuel assembly with a control ~~elements~~ rod assembly plus a ~~lifting~~handling tool (conservatively modeled as a total weight of 3,100 lb) from 36 inches above the top of the AP1000 Spent Fuel Storage Rack with subsequent impact on the edge of a cell;

2) A drop of a fuel assembly with a control ~~elements plus a lifting~~rod assembly plus a handling tool from 36 inches above the top of the rack down through an empty cell with impact on the rack baseplate away from the rack pedestal; and

3) A drop of a fuel assembly with a control ~~elements~~rod assembly plus a ~~lifting~~handling tool from 36 inches above the top of the rack down through an empty cell with impact on the rack baseplate directly above the rack pedestal.

All analyses were performed using the dynamic simulation code LS-DYNA (Reference 24). The impact velocity between the dropped fuel assembly and the rack was calculated by considering the resistance of the spent fuel pool water including the confinement effect of the rack cell. A finite element model of one-quarter of the spent fuel rack plus a single fuel assembly was modeled using appropriate shell and solid body elements available in LS-DYNA. The fuel assembly model, which is shown in Figure 2-9, consists of four parts: a rigid bottom end fitting, an elastic beam representing the fuel rods, a lumped mass at the top end of the beam representing the handling tool and control rod assembly, and a thin rigid shell that defines the enveloping size and shape of the fuel assembly. The mass and cross-sectional area properties of the elastic beam are based on the entire array of fuel rods (cladding material only). The fuel mass is lumped with the bottom end fitting. Appropriate non-linear material properties have been assigned to the rack components to permit yielding and permanent deformation to occur. Figures 2-10 and 2-11 show the details of the finite element model of the Region 1 spent fuel rack and Region 2 spent fuel rack, respectively.

For the drop to the top of the AP1000 Spent Fuel ~~Rack~~Storage Racks, the fuel assembly is assumed to strike the edge of an exterior cell at a speed corresponding to a 36-inch drop through water and to remain vertical as it is brought to a stop by the resisting members of the rack. The objective is to demonstrate that the extent of permanent damage to the impacted rack does not extend to the beginning of the active fuel region. For the AP1000 fuel, the active fuel region begins approximately 23.27 inches below the top of ~~either~~both the Region 1 or Region 2 racks.

For the drop through an empty cell to the baseplate, two extreme drop scenarios were considered in the analysis. The first scenario considered the maximum deformation of the rack baseplate by assuming that the impact occurs near the center of the rack. As the baseplate of the rack is connected to the cells by welding, a portion of the welding is expected to fail under this drop scenario. The energy from the falling fuel assembly is absorbed by weld failure plus deformation of the baseplate toward the floor. The fuel assemblies surrounding the impacted cell follows the baseplate deformation, and the objective is to determine how many fuel assemblies displace an amount sufficient to bring their active fuel region below the limit of the neutron absorbing material attached to each ~~fuel~~ rack cell wall. In the case of the AP1000 Spent Fuel Storage Racks, a 2-inch vertical movement of a fuel assembly, relative to the cell wall, will not require ~~any~~ a new criticality evaluation, because the neutron absorber material extends two inches below the active fuel region prior to any baseplate deformation. For the drop scenario where the impact occurs inside the empty cell directly above a rack pedestal, the spent fuel pool floor is ~~assumed to be~~ constructed using 4,000 psi concrete and the thickness of the spent fuel pool floor stainless steel liner is ~~assumed~~conservatively considered to be 3/16 inch thick, although the actual liner thickness is 1/2 inch. The objective of this impact analysis was to assess the damage in the rack pedestal and in the spent fuel pool floor and liner.

The results from the analyses are shown in Figures 2-12, 2-13, and 2-14:

- For the drop to the top of the ~~rack~~AP1000 Spent Fuel Storage Racks, the bounding damage occurs in the Region 2 rack with the extent of permanent damage limited to a depth of approximately 14.06 inches as shown in Figure 2-12. Therefore, the active fuel region remains surrounded by an undamaged cell wall and no further criticality evaluation is required.

- For the drop to the baseplate of the rack, the maximum baseplate deformation occurs in the Region 2 rack. Figure 2-13 shows that ~~nine fuel assemblies (including~~only the dropped fuel assembly~~) are~~ is moved downward more than 2 inches and ~~expose~~exposes active fuel on all ~~four~~ four sides. An additional ~~12~~ 8 fuel assemblies may drop a sufficient distance to expose active fuel on ~~2~~ two or three sides. This scenario is addressed in the criticality analysis.

- For the drop over a rack pedestal, the plastic strain in the spent fuel pool floor liner is shown in Figure 2-14. Since the liner strain remains elastic, the postulated drop event will not breach the spent fuel pool floor liner.

2.8.6 Stuck Fuel Assembly Evaluation

A nearly empty rack with one corner cell occupied is ~~subject~~subjected to an upward load of 5,000 lbf, which is assumed to be caused by the fuel sticking while being removed. The ramification of the loading is two-fold:

1. The upward load creates a force and a moment at the base of the rack;

2. The loading induces a local tension in the cell wall and shear stresses in the adjacent welds.

Strength of materials calculations have been performed to determine the maximum stress in the rack cell structure due to a postulated stuck fuel assembly. The results are summarized in Table 2-19, and show safety factors greater than 1.

2.9 CONCLUSIONS

From the results of the WPMR analyses, the following conclusions are made regarding the design and layout of the AP1000 Spent Fuel Storage Racks:

- All rack cell wall and pedestal stress factors are significantly below the allowable stress factor limit of 1.0.
- The worst-case compressive loads on the rack cellular structure during a seismic event are less that two thirds the critical buckling load.
- All weld stresses are below the allowable limits.
- A stuck fuel assembly results in stress conditions that are within the allowable limits.
- Fuel assembly drops were analyzed for each rack type. The drop onto the top of either the Region 1 or Region 2 racks is shown to be acceptable and does not require a criticality evaluation. The results of a dropped fuel assembly straight through an empty cell have been evaluated in the criticality analysis and have been found acceptable.

It is therefore considered demonstrated that the design of the AP1000 Spent Fuel Storage Racks meets the requirements for structural integrity for the postulated Level A and Level D conditions defined.

Table 2-1 Region 1 Spent Fuel Storage Rack Storage Cell Description	
(All dimensions are nominal and in inches; tolerances are not shown because they are Westinghouse Proprietary Information.)	
Parameter	**Value**
~~Storage~~ Cell Center-to-Center Pitch	10.93
~~Storage~~ Cell Inner Dimension (Width)	8.8
Inter-Cell Flux Trap Gap	1.644
~~Storage~~ Cell Length	199.5
~~Storage~~ Cell Wall Thickness	0.090
Neutron Absorber Dimensions (L x W x t)	172 x 7.5 x 0.106
Distance from Top of Rack Baseplate to Bottom of Neutron Absorber	6.23
Neutron Absorber Sheathing Thickness Internal Walls Periphery Walls	 0.035 0.075
~~Bumper Bar Length~~	~~15~~
~~Bumper Bar Thickness~~	~~0.5~~
~~Neutron Absorber Material~~	~~Metamic~~
~~Neutron Absorber Length~~	~~172~~
~~Neutron Absorber Width~~	~~7.5~~
~~Neutron Absorber Thickness~~	~~0.106~~
~~Neutron Absorber B_4C Loading~~	~~31 weight-percent~~
~~Baseplate Thickness~~	~~0.75~~
~~Baseplate Flow Hole Diameter~~	~~6~~
~~Rack Pedestal Type (fixed or adjustable)~~	~~Adjustable~~
~~Rack Pedestal Height (female + male)~~	~~2.75~~
~~Rack Female Pedestal Dimensions~~	~~20 x 20 x 2.25~~
~~Rack Male Pedestal Diameter~~	~~4.5~~
~~Rack Bearing Pad Thickness~~	~~1.5~~

Table 2-2 Region 2 Spent Fuel Storage Rack Storage Cell Description

(All dimensions are nominal and in inches; tolerances are not shown because they are Westinghouse Proprietary Information.)

Parameter	Value
~~Storage~~ Cell Center-to-Center Pitch	9.043
~~Storage~~ Cell Inner Dimension (Width)	8.8
Inter-Cell Flux Trap Gap	N/A
~~Storage~~ Cell Length	199.5
~~Storage~~ Cell Wall Thickness	0.090
Top of Cell Local Reinforcement Dimensions (L x W x t)	20.5 x 8.5 x 0.105
Neutron Absorber Dimensions (L x W x t)	172 x 7.5 x 0.106
Distance from Top of Rack Baseplate to Bottom of Neutron Absorber	6.23
Neutron Absorber Sheathing Thickness Internal Walls Periphery Walls	 0.035 0.075
~~Bumper Bar Length~~	~~15~~
~~Bumper Bar Thickness~~	~~0.5~~
~~Neutron Absorber Material~~	~~Metamic~~
~~Neutron Absorber Length~~	~~172~~
~~Neutron Absorber Width~~	~~7.5~~
~~Neutron Absorber Thickness~~	~~0.106~~
~~Neutron Absorber B_4C Loading~~	~~31 weight-percent~~
~~Baseplate Thickness~~	~~0.75~~
~~Baseplate Flow Hole Diameter~~	~~6~~
~~Rack Pedestal Type (fixed or adjustable)~~	~~Adjustable~~
~~Rack Pedestal Height (female + male)~~	~~2.75~~
~~Rack Female Pedestal Dimensions~~	~~18 x 18 x 2.25~~
~~Rack Male Pedestal Diameter~~	~~4.5~~
~~Rack Bearing Pad Thickness~~	~~1.5~~

Table 2-3 Defective Fuel Assembly Spent Fuel ~~Pool Damaged Fuel Assembly~~ Storage ~~Cells~~Rack Storage Cell Description	
(All dimensions nominal and are in inches; tolerances are not shown because they are Westinghouse Proprietary Information.)	
Parameter	**Value**
~~Storage~~ Cell Center-to-Center Pitch	11.65
~~Storage~~ Cell Inner Dimension (Width)	10.25
Inter-Cell Flux Trap Gap Between Defective Fuel Cells Defective Fuel Cells to Region 2 Cells	 0.91 1.644
~~Storage~~ Cell Length	199.5
~~Storage~~ Cell Wall Thickness	0.090
Neutron Absorber Dimensions (L x W x t)	172 x 7.5 x 0.106
Distance from Top of Rack Baseplate to Bottom of Neutron Absorber	6.23
Neutron Absorber Sheathing Thickness Internal Walls Periphery Walls	 0.035 0.075
~~Bumper Bar Length~~	~~15~~
~~Bumper Bar Thickness~~	~~0.5~~
~~Neutron Absorber Material~~	~~Metamic~~
~~Neutron Absorber Length~~	~~172~~
~~Neutron Absorber Width~~	~~7.5~~
~~Neutron Absorber Thickness~~	~~0.106~~
~~Neutron Absorber B_4C Loading~~	~~31 weight percent~~

Table 2-4 Simulations Listing

~~Run Number~~	~~Coefficient of Friction~~	~~Loading Configuration~~	~~Seismic Input (Floor Response Spectra)~~	~~Integration Time Step (sec)~~	~~Percentage of Calculated Stiffnesses~~
~~1~~	~~0.8~~	~~Fully Loaded~~	~~ASB99~~	~~1×10^{-5}~~	~~100%~~
~~2~~	~~0.5~~	~~Fully Loaded~~	~~ASB99~~	~~1×10^{-5}~~	~~100%~~
~~3~~	~~0.2~~	~~Fully Loaded~~	~~ASB99~~	~~1×10^{-5}~~	~~100%~~
~~4~~	~~0.8~~	~~Fully Loaded, Modified Gaps~~	~~ASB99~~	~~1×10^{-5}~~	~~100%~~
~~5~~	~~0.8~~	~~Mixed Loadings(1)~~	~~ASB99~~	~~1×10^{-5}~~	~~100%~~
~~6~~	~~0.8~~	~~Fully Loaded~~	~~ASB99~~	~~1×10^{-5}~~	~~80%~~
~~7~~	~~0.8~~	~~Fully Loaded~~	~~ASB99~~	~~1×10^{-5}~~	~~120%~~
~~8~~	~~0.8~~	~~Fully Loaded~~	~~ASB99~~	~~2.5×10^{-6}~~	~~100%~~
~~9~~	~~0.8~~	~~Empty~~	~~ASB99~~	~~1×10^{-5}~~	~~100%~~

Run Number	Coefficient of Friction	Loading Configuration	Integration Time Step (sec)	Percentage of Calculated Stiffnesses
1	0.8	Fully Loaded	1×10^{-5}	100%
2	0.5	Fully Loaded	1×10^{-5}	100%
3	0.2	Fully Loaded	1×10^{-5}	100%
4	0.8	Fully Loaded, Modified Gaps	1×10^{-5}	100%
5	0.8	Mixed Loadings(1)	1×10^{-5}	100%
6	0.8	Fully Loaded	1×10^{-5}	80%
7	0.8	Fully Loaded	1×10^{-5}	120%
8	0.8	Fully Loaded	2.5×10^{-6}	100%
9	0.8	Empty	1×10^{-5}	100%

Note:
1. See Figure 2-15 for the mixed loading layout configuration.

Table 2-5 Loading Combinations for AP1000 Spent Fuel Storage Racks

Loading Combination	Service Level
D + L D + L + T_o	Level A
D + L + T_a D + L + T_o +P_f	Level B
D + L + T_a +E'	Level D
D + L + F_d	The functional capability of the fuel racks should be demonstrated.

Notes:

1. There is no operating basis earthquake (OBE) for the AP1000 plant.
2. The AP1000 Spent Fuel Storage Racks are freestanding; thus, there is minimal or no restraint against free thermal expansion at the base of the rack. As a result, thermal loads applied to the rack (T_o and T_a) produce only local (secondary) stresses.

Abbreviations are those used in Reference 6:

D = Dead weight induced loads (including fuel assembly weight)

L = Live load (not applicable to fuel racks since there are no moving objects in the rack load path)

F_d = Force caused by the accidental drop of the heaviest load from the maximum possible height

P_f = Upward force on the racks caused by postulated stuck fuel assembly

E' = Safe Shutdown Earthquake (SSE)

T_o = Differential temperature induced loads based on the most critical transient or steady state condition under normal operation or shutdown conditions

T_a = Differential temperature induced loads based on the postulated abnormal design conditions

Table 2-6 Material Data (ASME – Section II, Part D)

Material	Young's Modulus E (psi)	Yield Strength S_y (psi)	Ultimate Strength S_u (psi)
Rack Material Data (200°F)			
SA-240, Type 304L[1]	27.6×10^6	21,300[2]	~~66,200~~ 66,100
Support Material Data (200°F)			
SA-240, Type 304L[1] (~~Upper part of support feet)~~Female pedestal)	27.6×10^6	21,300[2]	~~66,200~~ 66,100
SA-564, Type 630 (Hardened at 1100°-F) (Male pedestal)	~~28.5~~ 27.8 $\times 10^6$	106,300	140,000

Note:

1) The table includes material strength data for SA-240 Type 304L. Per Reference 9, the AP1000 Spent Fuel Storage Racks are fabricated from SA-240 Type 304, which has higher yield and ultimate strength values than SA-240 Type 304L. Unless otherwise noted, safety factors are calculated using the lesser properties of SA-240 Type 304L, as provided in this table, for conservatism.
   a) Section 2.3.4.3 includes a comparison to SA-240, Type 304 properties. At 200°F S_y= 25,000 and S_u=71,000.
   b) Section 2.8.2.3 uses SA-240, Type 304 properties at 150°F. For this case, S_y= 26,700 and S_u=73,000. It is acceptable to use this data because the racks are actually made out of 304, and the maximum normal spent fuel pool temperature is limited to 140°F.
2) Although the yield strength for SA-240, Type 304L at 200°F is 21,400 psi per Reference 14, the analyses conservatively use a yield strength of 21,300 psi, unless otherwise noted as discussed in note 1.

Table 2-7 AP1000 Spent Fuel Storage Rack~~s~~ Module and Fuel Data

Geometric Parameter	Dimension (in) Unless Noted
~~**Composite Box Data**~~	
~~Box ID~~	~~8.8~~
~~Pitch~~	~~10.93 (Region 1)~~ ~~9.043 (Region 2)~~
~~Wall Thickness~~	~~0.090~~
Rack Module Data	
~~Cell Length~~ Pedestal Type (fixed or adjustable)	~~199.5 (Region 1)~~ ~~199.5 (Region 2)~~Adjustable
~~Support~~Pedestal Height (female + male)	2.75
Female Pedestal ~~Side Dimension~~ Dimensions (L x W x t)	20~~.0~~ x 20~~.0~~ x 2.25 (Region 1) 18~~.0~~ x 18~~.0~~ x 2.25 (Region 2)
~~Female Pedestal Height~~	~~2.25~~
Male Pedestal Diameter	4.5
Bearing Pad Dimensions[1] (L x W x t)	12 x 12 x 1.5, 12 x 25 x 1.5, 25 x 25 x 1.5, or 25 x 32 x 1.5
Total Module Height	204.5
Bumper Bar Height	15
Bumper Bar Thickness	0.5
Baseplate Thickness	0.75
Baseplate Lateral Extension (beyond cell envelope)	~~7/8~~ 0.875 (on sides facing a Region 1 rack and on sides of a Region 1 rack that face a Region II rack) ~~1/2~~ 0.5 (on all other sides)
Fuel Data	
Minimum Dry Fuel Weight (excluding Control Components) (lb)	1,720 (Reference ~~20)~~42)
Maximum Dry Fuel Weight (including Control Components) (lb)	1,954 (References 42 and 20)
Minimum Nominal Fuel Assembly Size	8.404[2] (References ~~20~~ 42 and 43)
Maximum Nominal Fuel Assembly Size	8.426 (Reference ~~20)~~ 43)
Rack Details	

Rack	Array Size	Weight (lb)
A1, A2, A3	9 x 9	29,100
B1, B2, B3, B4	12 x 11	24,600

C1	12 x 10 (-2)	25,100

Note:

1) The bearing pad sizes vary by the location of the rack module within the pool. See Figure 2-1 to determine which bearing pad size is associated with each pedestal or group of neighboring pedestals.
2) The minimum nominal fuel assembly size excludes the IFM grids, which are located between the normal grid straps.

Table 2-8 Computer Codes Used for ~~AP1000 Spent Fuel Storage Racks Structural/Seismic~~ Analysis

Code	Version	Description
GENEQ	1.3	Generates artificial time histories from input response spectra set.
CORRE	1.3	Uses results from GENEQ and demonstrates required statistical independence of time histories.
PSD1	1.0	Uses results from GENEQ and compares regenerated Power Spectral Densities with target.
WORKING MODEL	2004	Is a Rigid Body Dynamics code used to improve baseline correction.
VMCHANGE	4.0	For a dry pool, develops a zero matrix of size = (number of racks x 22 DOF per rack).
MULTI1	1.55	Incorporates appropriate non-zero values due to structural effects that are put in appropriate locations in the output matrix from VMCHANGE to form the final mass matrix for the analysis. The appropriate non-zero right-hand sides are also developed.
MASSINV	2.1	Calculates the inverse of the mass matrix.
MSREFINE	2.1	Refines the inverse of the mass matrix.
PREDYNA1	1.5	Generates various input lines for the input file required to run the dynamic solver.
PD16	2.1	Generates rack-to-fuel compression-only impact springs, rack-to-ground impact springs, and rack elastic deflection springs for each rack being analyzed and creates the appropriate lines of input for the solver.
SPG16	3.0	Generates compression-only rack-to-rack impact springs for the specific rack configuration in the pool for the solver.
MR216	2.0	Is a solver for the dynamic analysis of the racks; uses an input file from the cumulative output from PREDYNA, PD16, and SPG16, together with the mass matrix, right-hand side matrix, and the final time histories from GENEQ.
DYNAPOST	2.0	Post-Processor for MR216; generates safety factors, maximum pedestal forces, and maximum rack movements.
ANSYS	9.0	Is a general purpose commercial FEA code.
LS-DYNA	970	General purpose commercial FEA code optimized for shock and impact analyses.

~~Table 2-9 Results Summary~~

~~Run No.~~	~~Coefficient of Friction~~	~~Max. Stress Factor~~	~~Max. Vertical Load (lbf)~~	~~Max. Shear Load (lbf) (X or Y)~~	~~Max. Fuel-to-Cell Wall Impact (lbf)~~
~~1~~	~~0.8~~	~~0.386~~	~~360,000~~	~~176,000~~	~~1,409~~

~~2~~	~~0.5~~	~~0.393~~	~~364,000~~	~~142,000~~	~~1,417~~
~~3~~	~~0.2~~	~~0.382~~	~~359,000~~	~~68,300~~	~~1,420~~
~~4~~	~~0.8~~	~~0.403 (+4.4%)~~	~~366,000 (+1.7%)~~	~~225,000 (+27.8%)~~	~~1,420 (+0.8%)~~
~~5~~	~~0.8~~	~~0.361 (-6.5%)~~	~~292,000 (-18.9%)~~	~~125,000 (-29.0%)~~	~~1,076 (-23.6%)~~
~~6~~	~~0.8~~	~~0.414 (+7.3%)~~	~~403,000 (+11.9%)~~	~~167,000 (-5.1%)~~	~~1,370 (-2.8%)~~
~~7~~	~~0.8~~	~~0.434 (+12.4%)~~	~~404,000 (+12.2%)~~	~~219,000 (+24.4%)~~	~~1,455 (+3.3%)~~
~~8~~	~~0.8~~	~~0.401 (+3.9%)~~	~~364,000 (+1.1%)~~	~~194,000 (+10.2%)~~	~~1,417 (+0.6%)~~
~~9~~	~~0.8~~	~~0.068~~	~~61,200~~	~~19,800~~	~~0~~

Table 2-9 Results Summary[1]

Run No.	Max. Stress Factor	Max. Vertical Load (lbf)	Max. Shear Load (X or Y) (lbf)	Max. Fuel-to-Cell Wall Impact (lbf)	Max. Baseplate Displacement (in)	Max. Top Displacement (in)	Max. Rack-to-Wall Impact (lbf)
1	0.386 (0.338)	360,000 (280,000)	176,000 (150,000)	1,409 (1,235)	0.25 (0.04)	3.99 (1.00)	328,600 (116,500)
2	0.393 (0.336)	364,000 (278,000)	142,000 (108,000)	1,417 (1,167)	0.15 (0.05)	2.32 (1.14)	242,000 (122,900)
3	0.382 (0.277)	359,000 (245,000)	68,300 (48,600)	1,420 (1,280)	1.15 (0.54)	1.41 (0.81)	89,500 (27,800)
4	0.403 (0.359)	366,000 (340,000)	225,000 (141,000)	1,420 (1,191)	0.08 (0.06)	3.45 (1.68)	295,300 (128,900)
5	0.361 (0.278)	292,000 (246,000)	125,000 (99,300)	1,076 (892)	0.91 (1.06)	1.90 (1.40)	258,700 (99,000)
6	0.414 (0.355)	403,000 (316,000)	167,000 (142,000)	1,370 (1,189)	0.14 (0.05)	3.53 (1.45)	312,600 (173,000)
7	0.434 (0.348)	404,000 (312,000)	219,000 (161,000)	1,455 (1,296)	0.21 (0.05)	2.73 (2.11)	289,700 (242,400)
8	0.401 (0.338)	364,000 (284,000)	194,000 (125,000)	1,417 (1,068)	0.18 (0.03)	2.65 (0.92)	322,500 (176,300)
9	0.068 (0.068)	61,200 (61,200)	19,800 (20,300)	0 (0)	0.02 (0.01)	0.46 (0.21)	0 (0)

Notes:

1. For information, the results from the simulations using the new seismic input that was made available in May 2010 via Reference 37 are included in this table in parenthesis after the results from the design basis runs that use the seismic input that was transmitted to Holtec International via Reference 19. A comparison of the overall maximum loads that resulted from the most severe case of all of the simulations using each set of seismic input is as follows:

Seismic Input	Max. Stress Factor	Max. Pedestal Stress Factor	Max. Vertical Load	Max. Shear Load	Max. Fuel-to-Cell Wall Impact	Max. Baseplate Displacement	Max. Top of Rack Displacement	Max. Rack-to-Wall Impact
Design Basis (Ref. 19 & 36)	0.434	0.102	404,000	225,000	1,455	1.15	3.99	328,600
Updated Data (Ref. 37 & 39)	0.359	0.080	340,000	161,000	1,296	1.05	2.11	242,400
% Difference	-17.3	-21.6	-15.8	-28.4	-10.9	-7.8	-47.1	-26.2

Table 2-10 Deleted (combined with Table 2-9)

Table 2-11 Maximum Pedestal and Cell Wall Stress Factors

Run Number	Pedestal Stress Factor	Cell Wall Stress Factor
1	0.092	$\left(0.386 \times \frac{1}{0.701}\right)^{0.386} = 0.551$ *
2	0.091	$\left(0.393 \times \frac{1}{0.681}\right)^{0.393} = 0.577$ *
3	0.082	$\left(0.382 \times \frac{1}{0.681}\right)^{0.382} = 0.561$ *
4	0.102	$\left(0.403 \times \frac{1}{0.701}\right)^{0.403} = 0.575$ *
5	0.076	$\left(0.361 \times \frac{1}{0.701}\right)^{0.361} = 0.515$ *
6	0.097	$\left(0.414 \times \frac{1}{0.681}\right)^{0.414} = 0.608$ *
7	0.100	$\left(0.434 \times \frac{1}{0.681}\right)^{0.434} = 0.637$ *
8	0.095	$\left(0.401 \times \frac{1}{0.701}\right)^{0.401} = 0.572$ *
9	0.012	$\left(0.068 \times \frac{1}{0.701}\right)^{0.068} = 0.097$ *

Note:
* Adjustment factor accounting for ASME Code Slenderness Ratio

Table 2-12 Baseplate-to-Cell Weld Maximum ~~Weld~~ Stresses[1]

~~Weld Stress (psi)~~	~~Allowable Stress (psi)~~	~~Safety Factor~~
~~28,943~~	~~35,748~~	~~1.24~~

Stress Type	Stress (psi)	Allowable Stress (psi)	Safety Factor
Weld Stress	23,157	35,694	1.54
Cell Base Metal Shear Stress	16,374	18,000	1.10

Note:
1. The shear stress in the baseplate base metal is not specifically evaluated due to the robustness of the baseplate.

Table 2-13 Deleted

Table 2-14 Baseplate-to-Pedestal -Weld Maximum ~~Weld~~ Stresses[1]

~~Weld Stress (psi)~~	~~Run No.~~	~~Allowable Stress (psi)~~	~~Safety Factor~~
~~12,516~~	~~4~~	~~35,748~~	~~2.86~~

Weld Stress (psi)	Allowable Stress (psi)	Safety Factor
12,516	35,694	2.85

Note:
1. The shear stress in the base metal for the baseplate and the pedestal is not specifically evaluated due to the robustness of these items.

Table 2-15 Pedestal Thread Shear Stress

Base Metal Shear Stress (psi)	Allowable Stress (psi)	Safety Factor
17,501	19,224*	1.10

Note:
* Based on yield strength of SA-240 Type 304 at 150°F (0.72 x 26,700 psi = 19,224 psi).

Table 2-16 Cell-to-Cell Weld Maximum ~~Weld~~ Stresses

Stress Type	Stress (psi)	Allowable Stress (psi)	Safety Factor
Weld Stress	13,121	~~35,748~~ 35,694	2.72
Base Metal Shear Stress	9,278	15,336	1.65

Table 2-17 Deleted

Table 2-18 Degrees of Freedom for Single Rack Dynamic Model

Location (Node)	Displacement			Rotation		
	U_x	U_y	U_z	θ_x	θ_y	θ_z
1	p_1	p_2	p_3	q_4	q_5	q_6
2	p_7	p_8	p_9	q_{10}	q_{11}	q_{12}
Node 1 is assumed to be attached to the rack at the bottom most point. Node 2 is assumed to be attached to the rack at the top most point. Refer to Figure 2-4 for node identification.						
2^*	p_{13}	p_{14}				
3^*	p_{15}	p_{16}				
4^*	p_{17}	p_{18}				
5^*	p_{19}	p_{20}				
1^*	p_{21}	p_{22}				

where the relative displacement variables q_i are defined as:

$p_i = q_i(t) + U_x(t)$ $\quad i = 1,7,13,15,17,19,21$

$= q_i(t) + U_y(t)$ $\quad i = 2,8,14,16,18,20,22$

$= q_i(t) + U_z(t)$ $\quad i = 3,9$

$= q_i(t)$ $\quad i = 4,5,6,10,11,12$

p_i denotes absolute displacement (or rotation) with respect to inertial space

q_i denotes relative displacement (or rotation) with respect to the pool floor ~~slab~~

* denotes fuel mass nodes

U(t) are the three known earthquake displacements

Table 2-19 Results from Stuck Fuel Assembly Evaluation

Item	Calculated Stress (psi)	Allowable Stress (psi)	Safety Factor
Cell Wall Tensile Stress ~~in Cell Wall~~	4,805	12,780*	2.66
~~Shear Stress in~~ Cell-to-Cell Weld Shear Stress	9,428	~~19,860~~ 19,830	~~2.11~~ 2.10
Base Metal Shear Stress ~~in Base Metal~~	6,667	8,520	1.28

Note:

* Conservatively based on Level A limit for tensile stress (0.6 Sy). Stuck fuel assembly load is defined as Service Level B per Table 2-5.

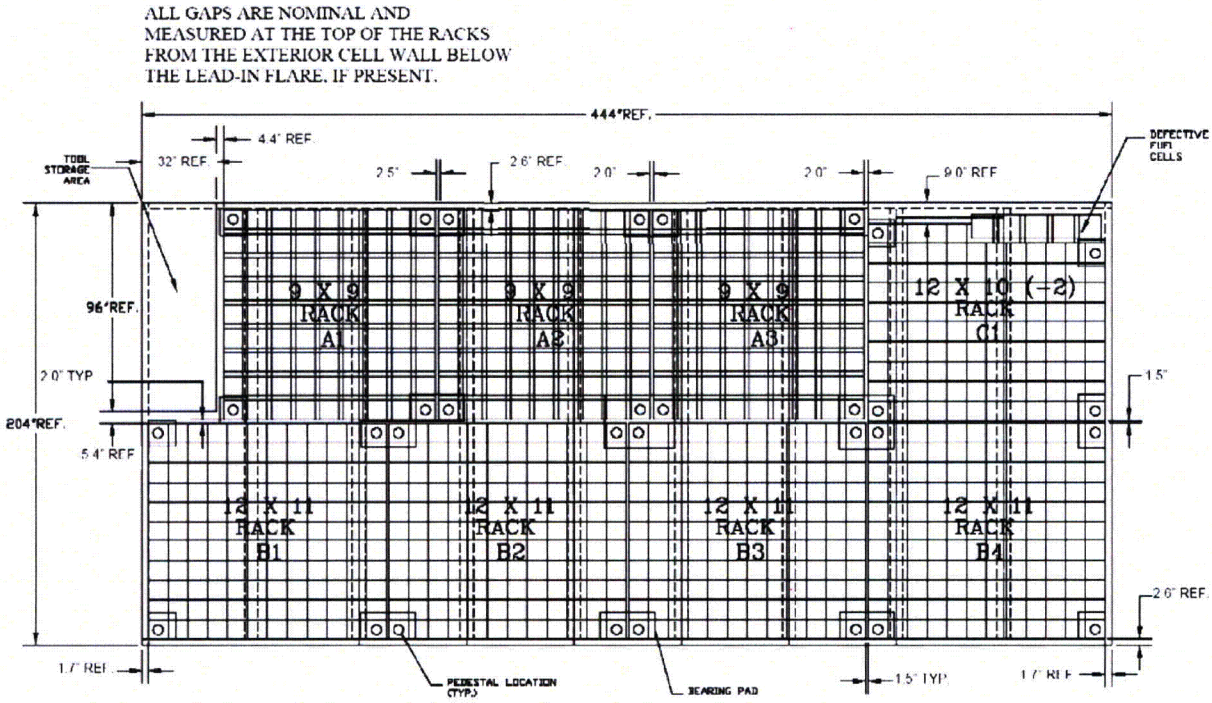

889 Total Storage Locations
Leak Chases Shown in Phantom

Figure 2-1 Spent Fuel Pool Storage Layout ~~(889 Total Storage Locations) Leak Chases Show in Phantom~~

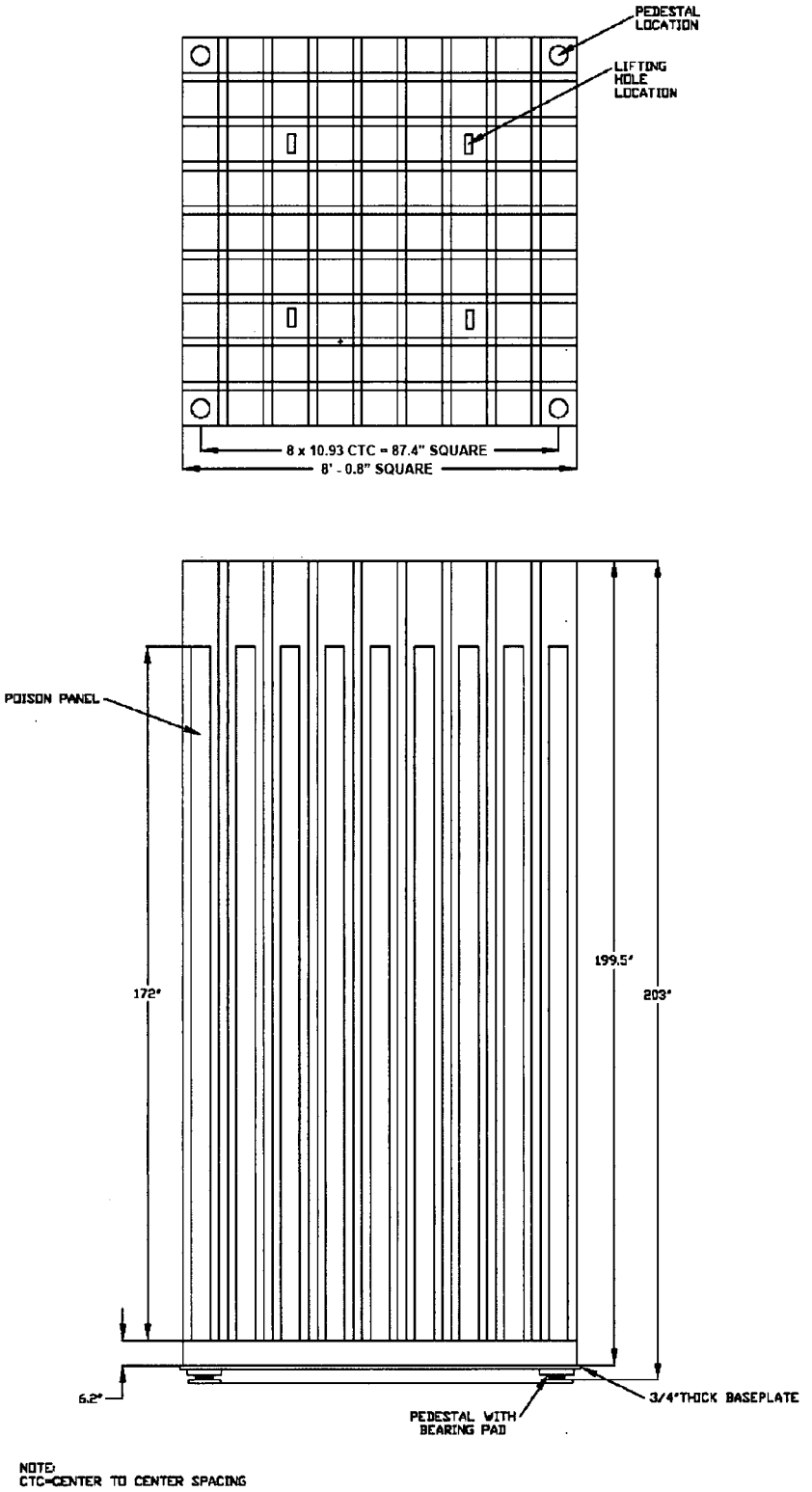

Figure 2-2 Configuration of a Region 1 Storage Rack (Sheet 1 of 2)

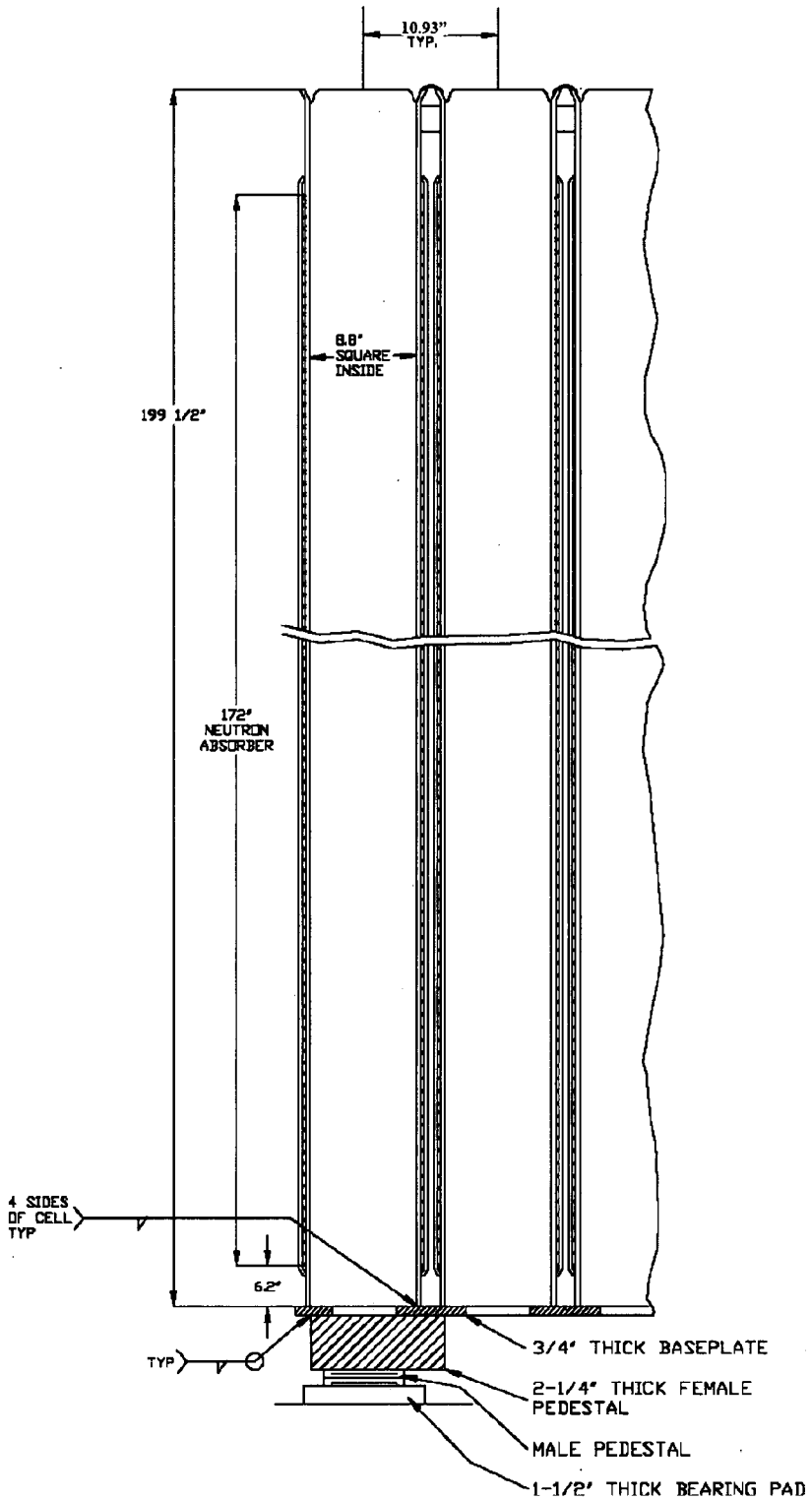

Figure 2-2 Configuration of a Region 1 Storage Rack (Sheet 2 of 2)

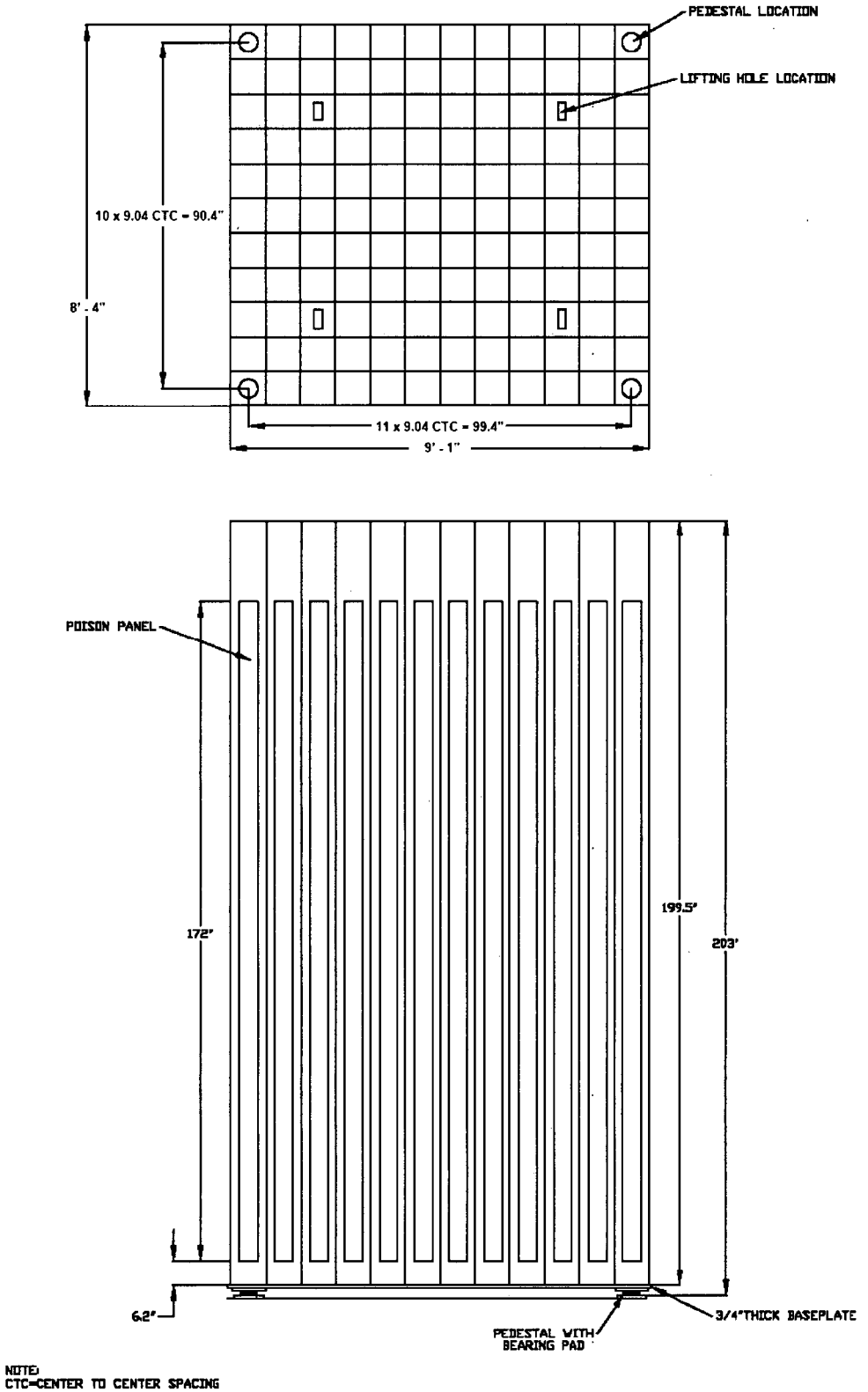

Figure 2-3 Configuration of a Region 2 Storage Rack (Sheet 1 of 2)

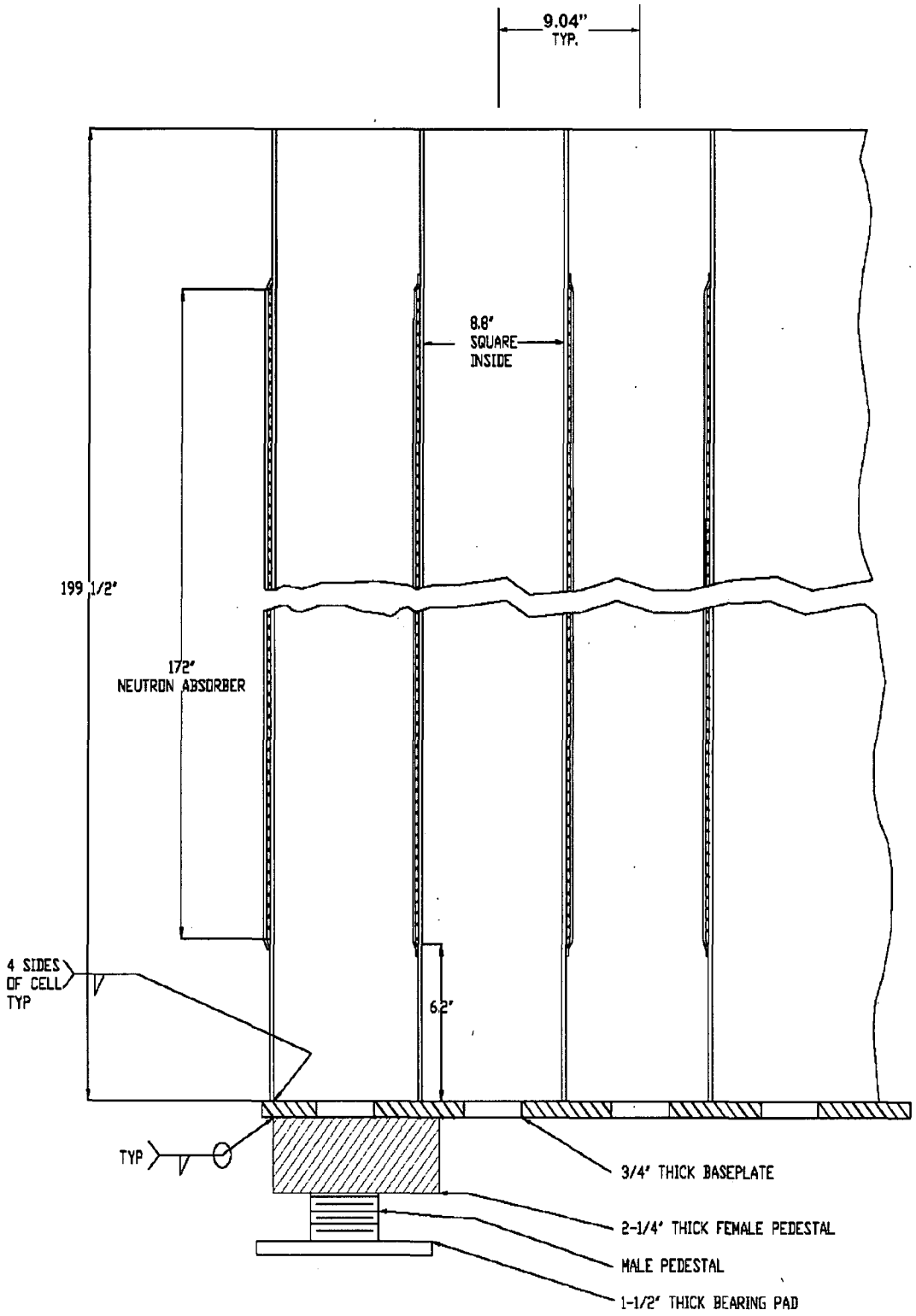

Figure 2-3 Configuration of a Region 2 Storage Rack (Sheet 2 of 2)

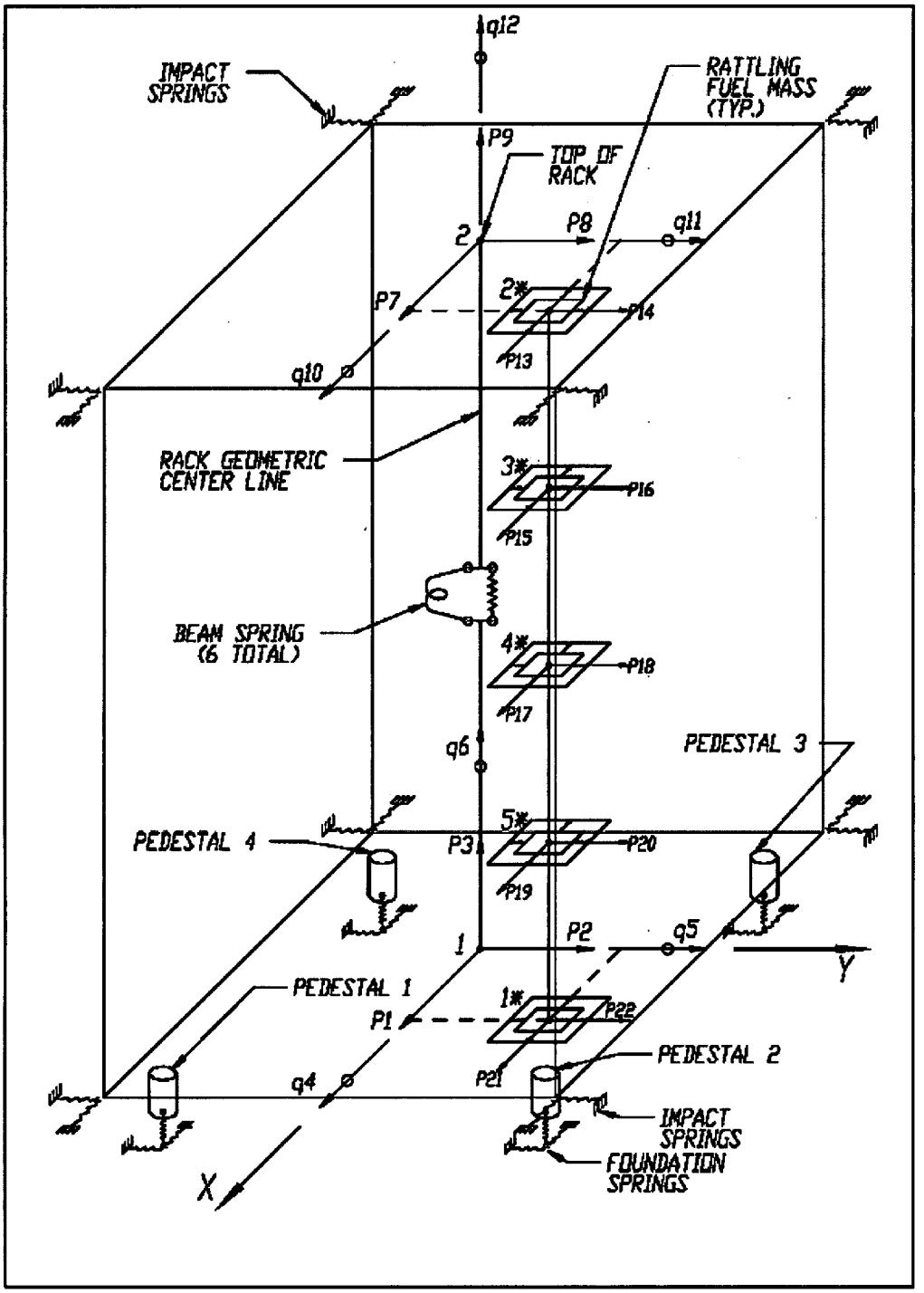

Figure 2-4 Schematic Diagram of Dynamic Model for DYNARACK

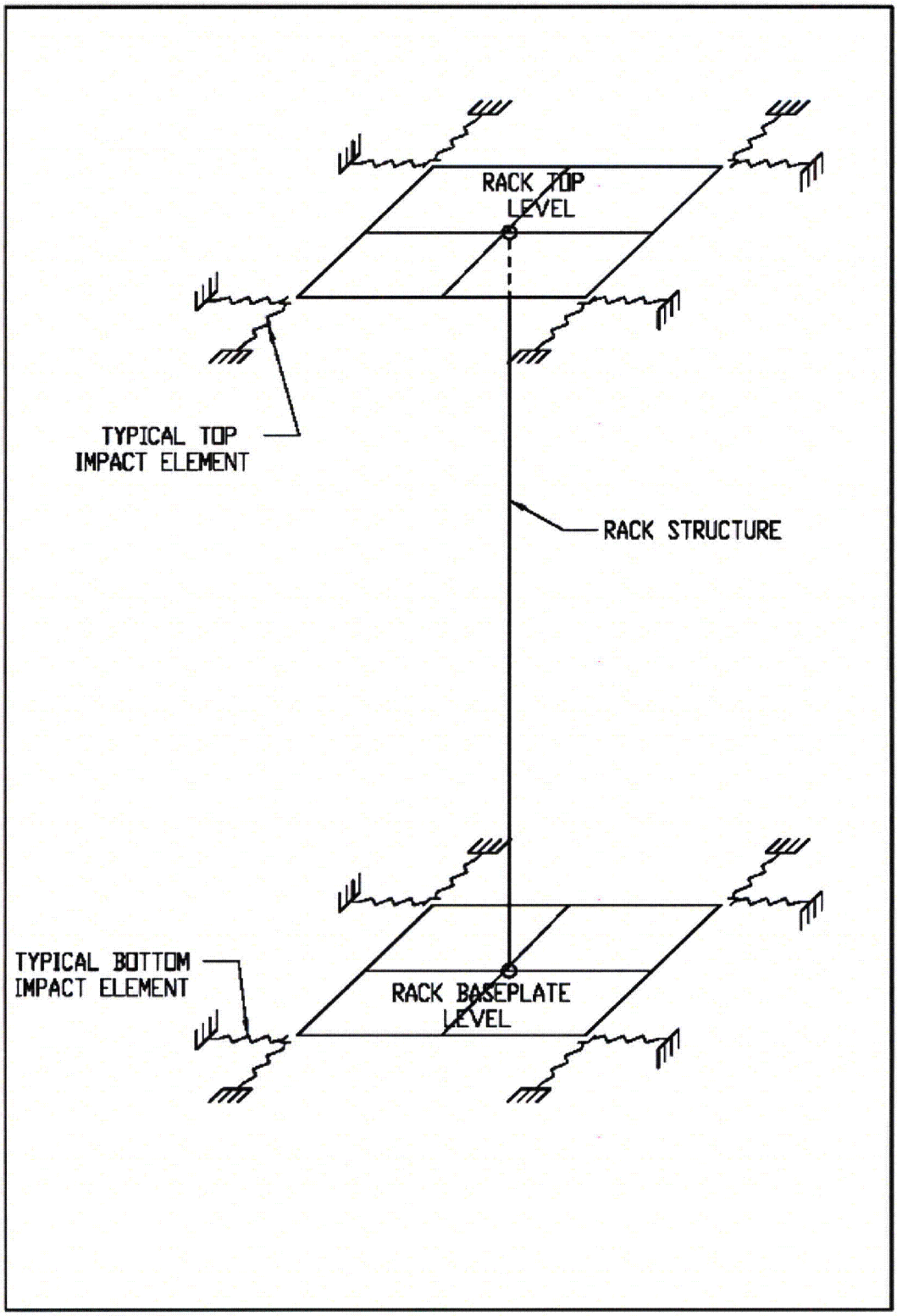

Figure 2-5 Rack-to-Rack or Wall Impact Springs

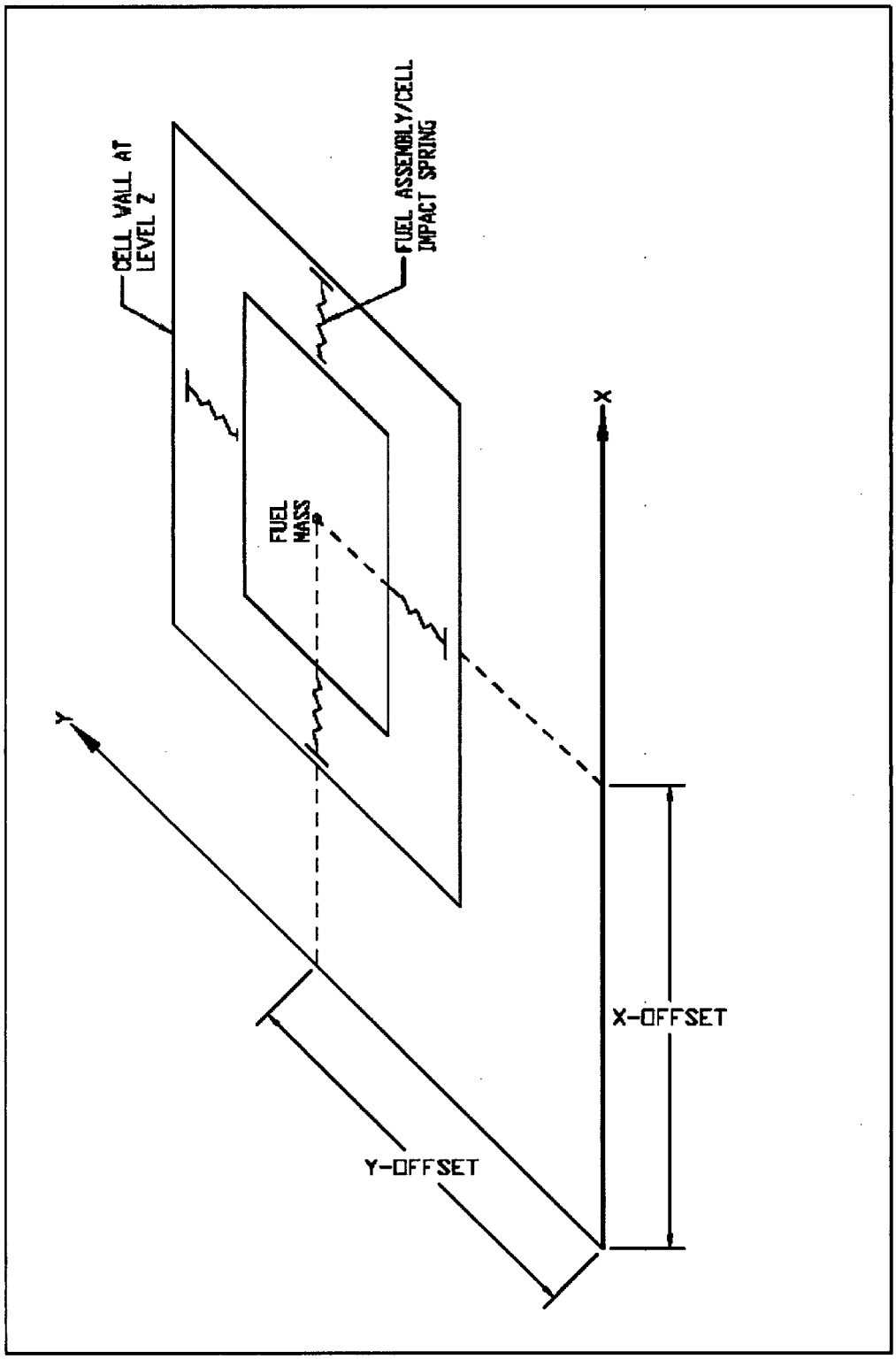

Figure 2-6 Fuel-to-Rack Impact Springs at Level of Rattling Mass

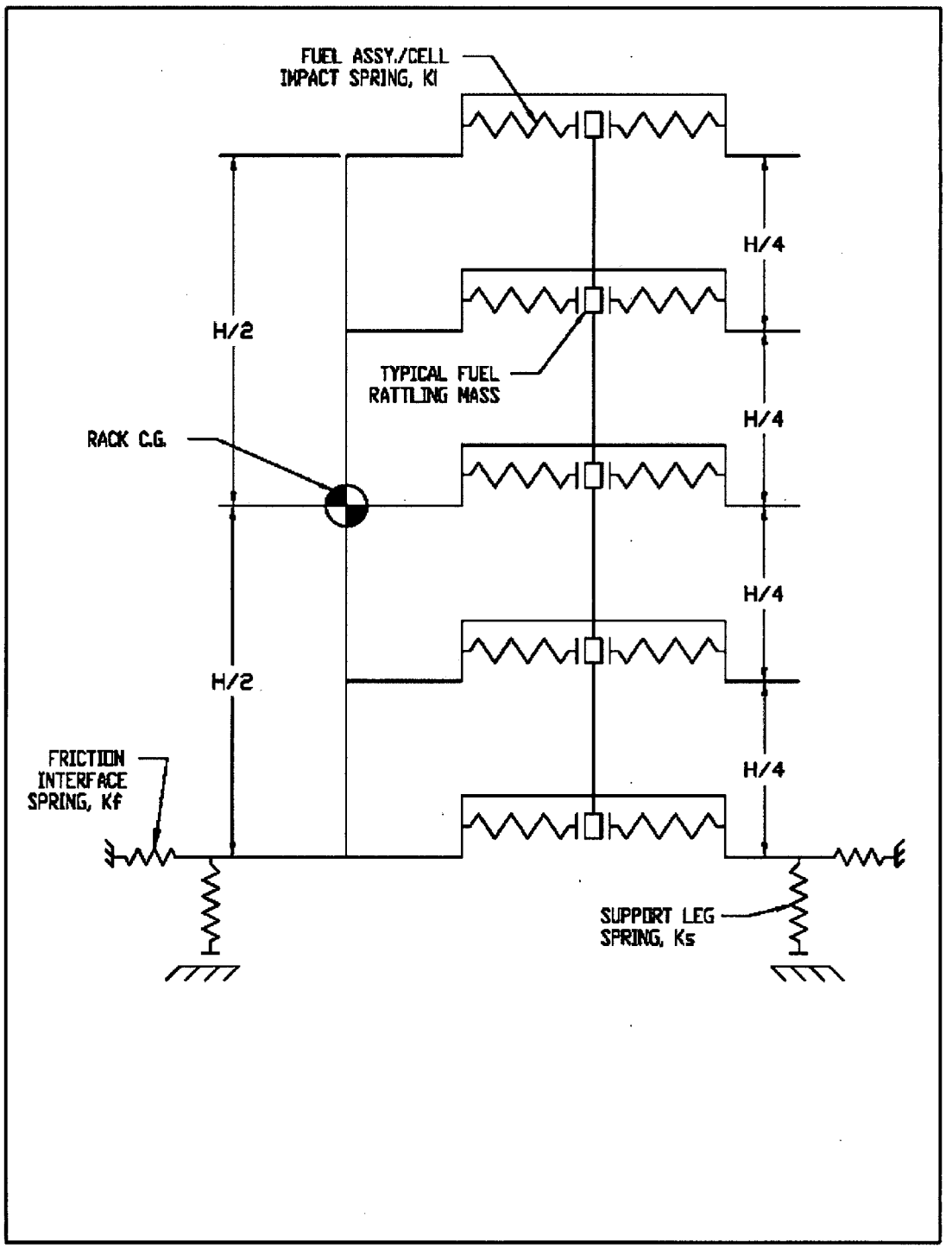

Figure 2-7 Two-Dimensional View of Spring-Mass Simulation

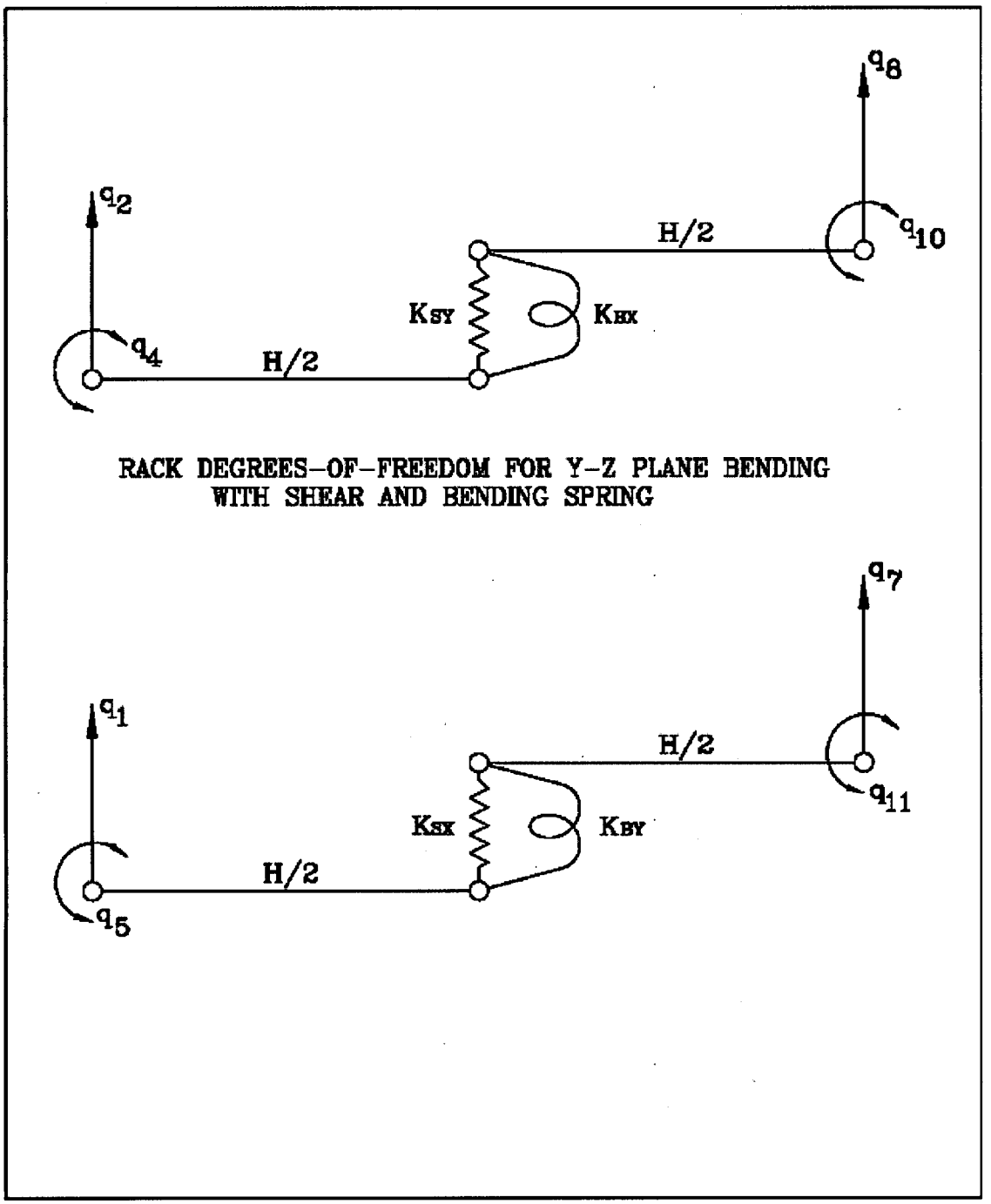

Figure 2-8 Rack Degrees-of-Freedom for X-Y Plane Bending with Shear and Bending Spring

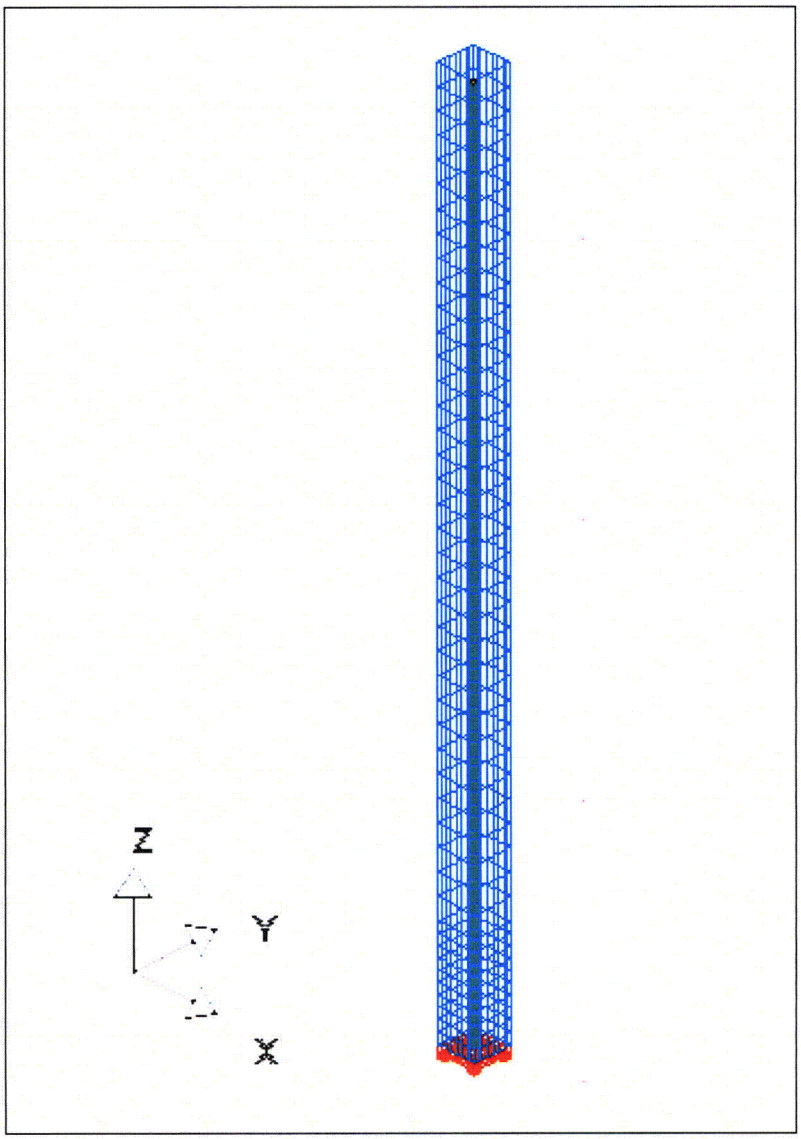

Figure 2-9 LS-DYNA Model of Dropped Fuel Assembly

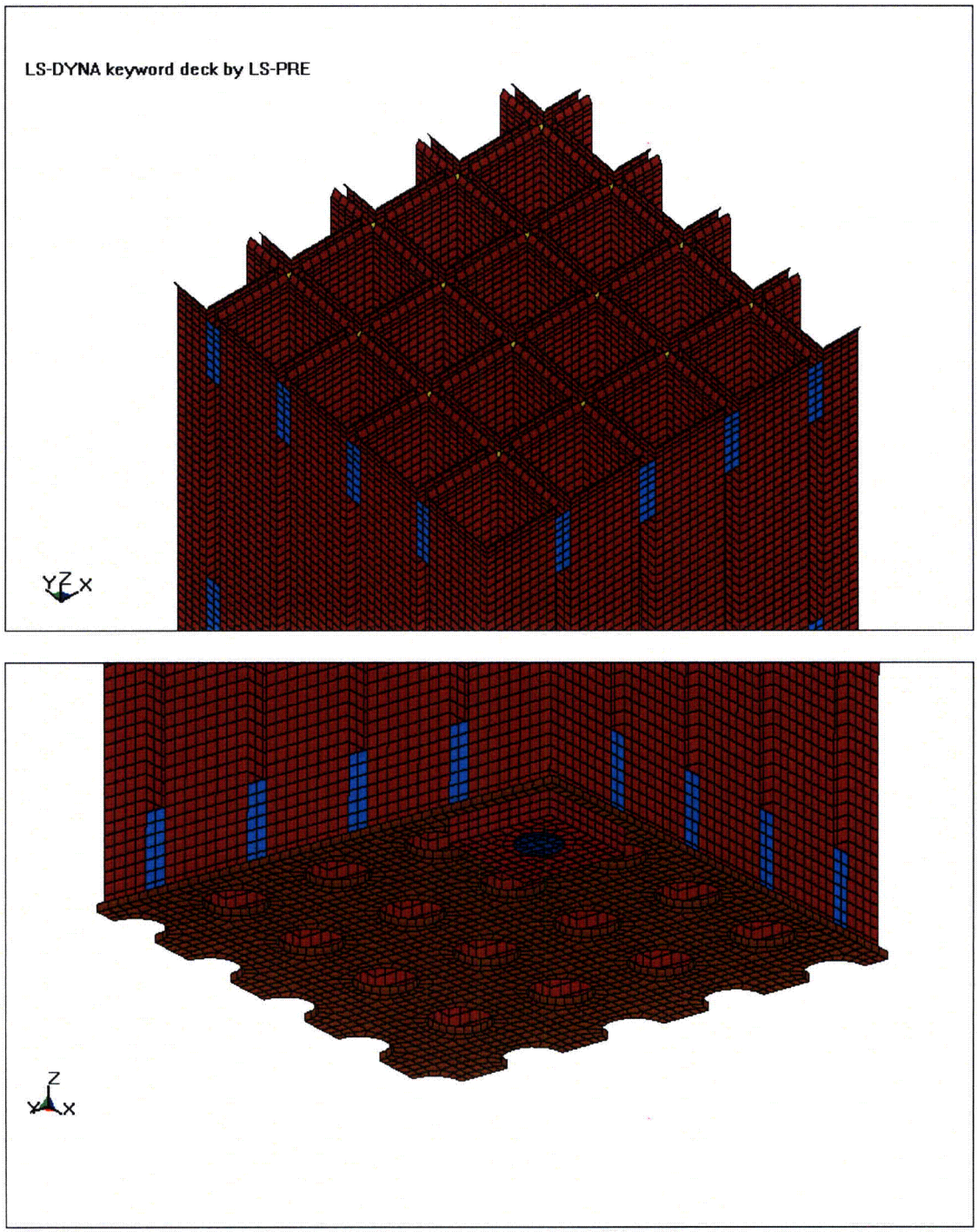

Figure 2-10 LS-DYNA Model of Top and Bottom of AP1000 Region 1 Spent Fuel Rack

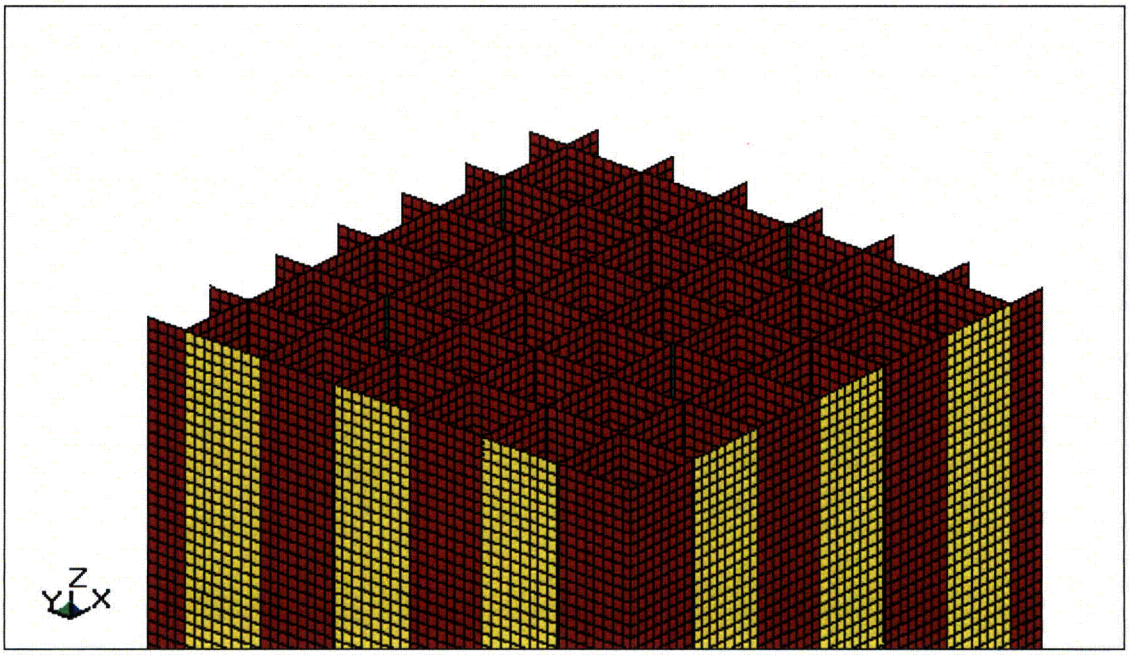

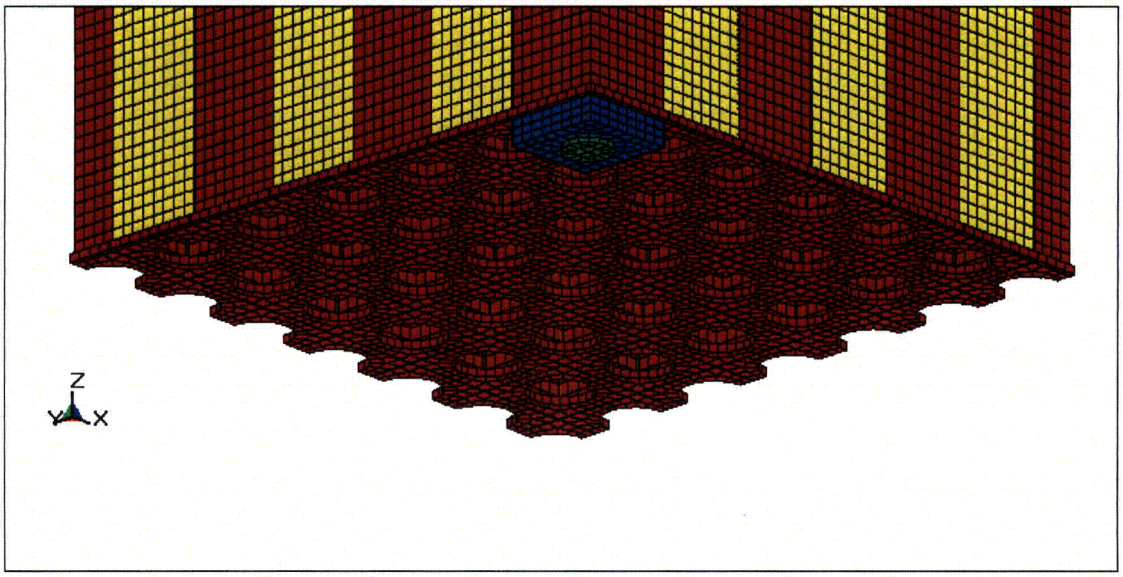

Figure 2-11 LS-DYNA Model of Top and Bottom of AP1000 Region 2 Spent Fuel Rack

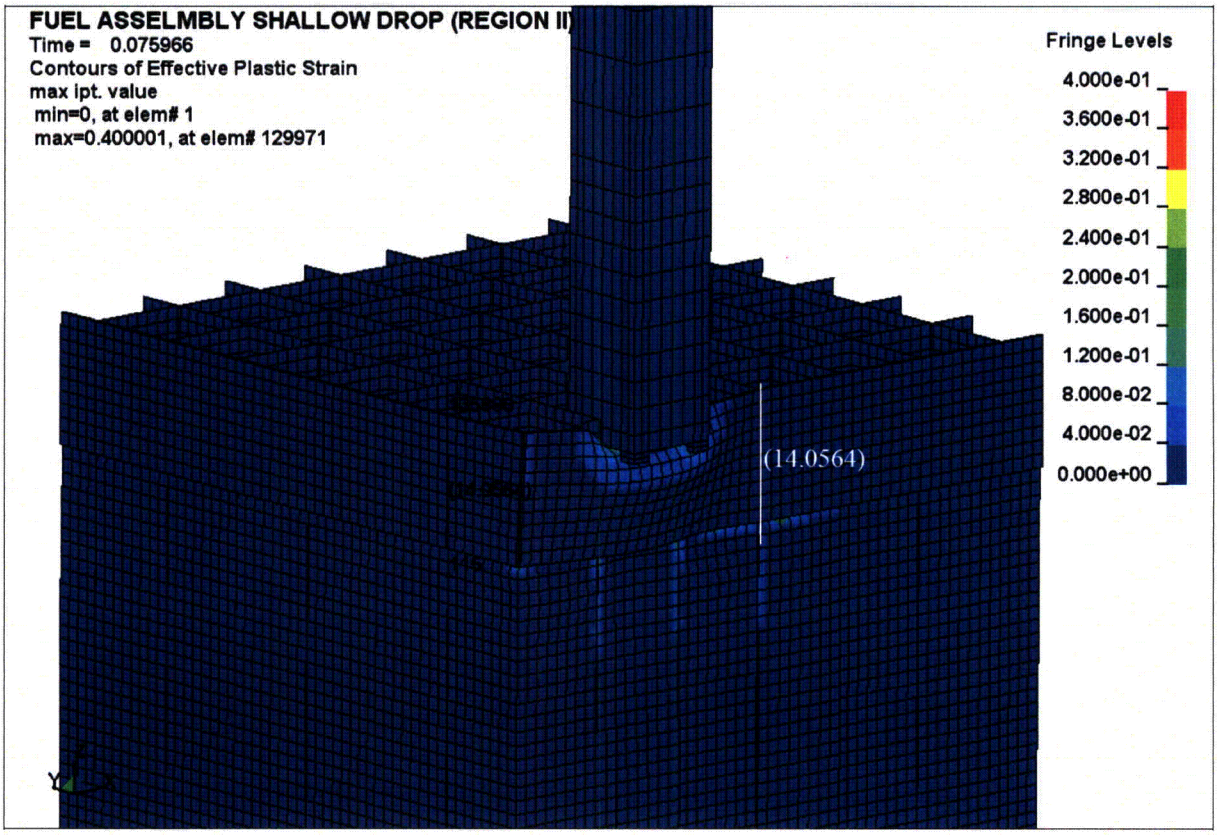

Figure 2-12 Plastic Strain Results from Drop to Top of Region 2 Spent Fuel Rack

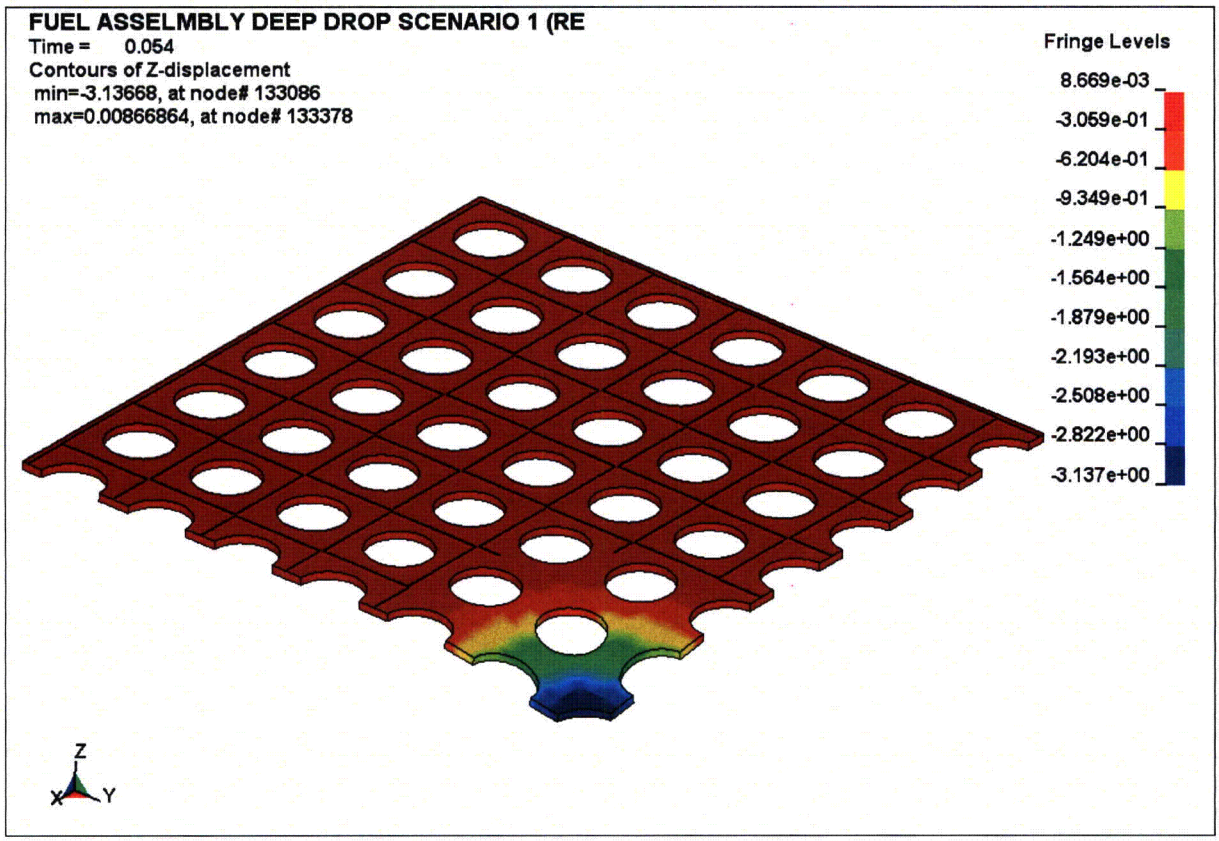

Figure 2-13 Maximum Rack Baseplate Deformation from Drop into an Empty Cell
~~(One-Quarter of Impact Zone Shown)~~

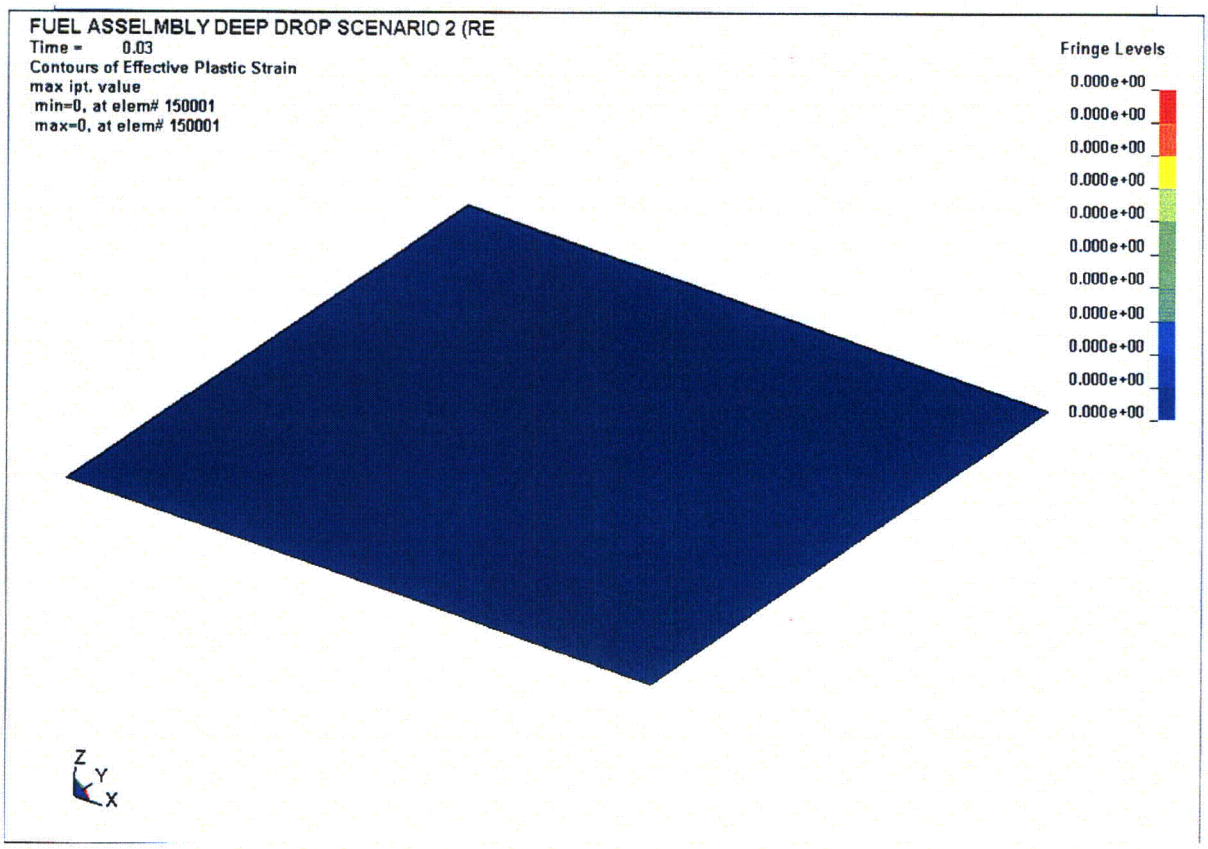

Figure 2-14 Plastic Strain in Pool Liner from Drop over Rack Pedestal

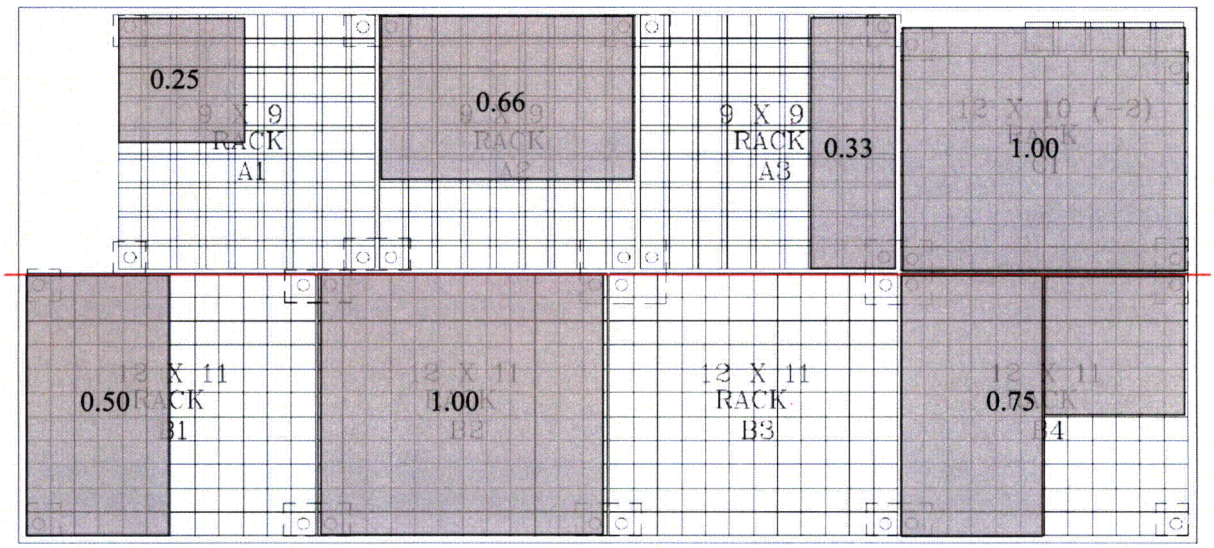
0.25
9 X 9
RACK
A1
0.66
9 X 9
RACK
A2
9 X 9
RACK
A3
0.33
12 X 10 (-2)
1.00
0.50
12 X 11
RACK
B1
1.00
12 X 11
RACK
B2
12 X 11
RACK
B3
0.75
12 X 11
RACK
B4

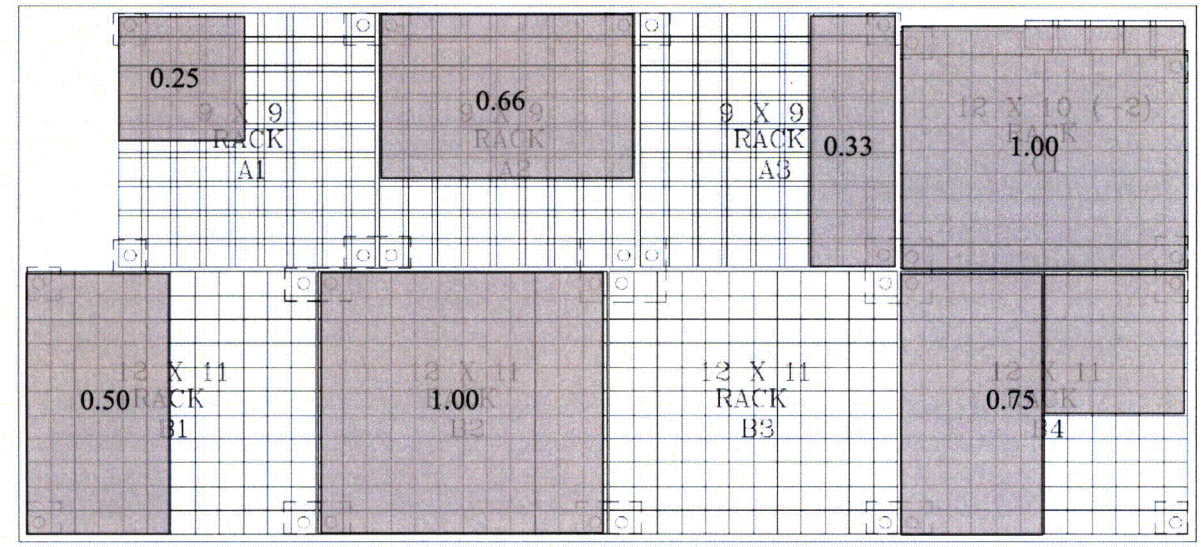
0.25
9 X 9
RACK
A1
0.66
9 X 9
RACK
A2
9 X 9
RACK
A3
0.33
12 X 10 (-2)
1.00
0.50
12 X 11
RACK
B1
1.00
12 X 11
RACK
B2
12 X 11
RACK
B3
0.75
12 X 11
RACK
B4

Figure 2-15: Loading Pattern for Run Number 5 - Mixed Loading Case

3 REGULATORY IMPACT

The structural/seismic analysis of the AP1000 Spent Fuel Storage Racks is addressed in subsection 9.1.2.2.1, "Spent Fuel Storage" of the NRC Final Safety Evaluation Report (Reference 2). The completion of the structural/seismic analysis for the AP1000 Spent Fuel Storage Racks is identified in the Final Safety Evaluation Report as COL Action Item 9.1.6-3.

~~The changes to the DCD presented in this report do not represent an adverse change to the design functions of the AP1000 Spent Fuel Storage Racks, or to how design functions are performed or controlled. From a thermal perspective, the Spent Fuel Pool Cooling System has the capability to cool the fully loaded spent fuel pool (889 fuel assemblies) under the design basis conditions. The structural/seismic analysis of the AP1000 Spent Fuel Storage Racks is consistent with the description of the analysis in subsection 9.1.2.2.1, "Spent Fuel Rack Design," of the DCD. Therefore, the changes to the DCD do not involve revising or replacing a DCD-described evaluation methodology. The changes to the DCD do not involve a test or experiment not described in the DCD. The DCD change does not require a license amendment per the criteria of VIII.B.5.b. of Appendix D to 10 CFR Part 52.~~

~~None of the changes described involve design features used to mitigate severe accidents. Therefore, a license amendment based on the criteria of VIII.B.5.c of Appendix D to 10 CFR Part 52 is not required.~~

There are no DCD changes presented in this report that represent an adverse change to the design functions of the AP1000 Spent Fuel Storage Racks, or to how design functions are performed or controlled. The structural/seismic analysis of the AP1000 Spent Fuel Storage Racks is consistent with the description of the analysis in subsection 9.1.2.2.1, "Spent Fuel Rack Design," of the DCD. There are no DCD changes that involve revising or replacing a DCD-described evaluation methodology, or a test or experiment. Nor are there any DCD changes that require a license amendment per the criteria of VIII.B.5.b. of Appendix D to 10 CFR Part 52.

There are no DCD changes that involve design features used to mitigate severe accidents. Therefore, a license amendment based on the criteria of VIII.B.5.c of Appendix D to 10 CFR Part 52 is not required.

The closure of the COL Information Item will not alter barriers or alarms that control access to protected areas of the plant. The closure of the COL Information Item will not alter requirements for security personnel. Therefore, the closure of the COL Information Item does not have an adverse impact on the security assessment of the AP1000.

4 REFERENCES

1. APP-GW-GL-700, AP1000 Design Control Document, Rev. ~~16~~ 17.

2. Final Safety Evaluation Report Related to Certification of the AP1000 Standard Design, September 2004.

3. Westinghouse Calculation, APP-FS02-S3C-002, Rev. ~~2~~ 3, "AP1000 Spent Fuel Storage Racks Structural/Seismic Analysis," ~~November 2009.~~May 2010. (Westinghouse Proprietary)

4. Deleted

5. Deleted

6. U.S. NRC Standard Review Plan NUREG-0800, SRP 3.8.4, Rev. 1, Appendix D, "Technical Position on Spent Fuel Pool Racks," July 1981.

7. ~~-~~Paul, B., "Fluid Coupling in Fuel Racks: Correlation of Theory and Experiment," NUSCO/Holtec Report HI-88243. (Holtec Proprietary)

8. U.S. NRC Standard Review Plan, NUREG-0800 (SRP 3.7.1, Rev. 2), March 1997.

9. Westinghouse Documents: APP-FS02-V1-001, APP-FS02-V2-002, APP-FS02-V2-003, APP-FS02-V2-004, APP-FS02-V2-005, APP-FS02-V6-006, APP-FS02-V6-007, APP-FS02-V6-008, and APP-FS02-V6-009, "Discrete Zone Two Region Spent Fuel Rack Pool Layout," all Rev. ~~2, November 2009.~~3, May 2010. (Westinghouse Proprietary)

10. Soler, A.I. and Singh, K.P., "Seismic Responses of Free Standing Fuel Rack Constructions to 3-D Motions," Nuclear Engineering and Design, Vol. 80, pp. 315-329 (1984).

11. Levy, S., and Wilkinson, John, "The Component Element Method in Dynamics," McGraw Hill, 1976.

12. ASME Boiler & Pressure Vessel Code, Section III, Subsection NF, 1998 Edition with 2000 Addenda.

13. Holtec Computer Code MR216 (multi-rack transient analysis code, a.k.a. DYNARACK), Version 2.00. QA documentation contained in Holtec Report HI-92844. (Holtec Proprietary)

14. ASME Boiler & Pressure Vessel Code, Section II, Part D, 1998 Edition with 2000 Addenda.

15. Holtec Computer Code DYNAPOST (Analysis Post Processor), v. 2.0. (Holtec Proprietary)

16. Fritz, R.J., "The Effects of Liquids on the Dynamic Motions of Immersed Solids," Journal of Engineering for Industry, Trans. of the ASME, February 1972, pp. 167-172.

17. Deleted

18. Deleted

19. AP1000 Letter Number DCP/HII0012 "Input Spectra for Revised Spent Fuel Rack Analysis," from J.M. Iacovino (Westinghouse Electric Company) to Mr. Evan Rosenbaum (Holtec International), Dated October 18, 2007. (Westinghouse Proprietary)

20. Westinghouse Document: APP-RXS-M8-020, Rev. 1, "AP1000 NSSS / Core Design Interface Document," March 2009. (Westinghouse Proprietary)

21. Rabinowicz, E., "Friction Coefficients of Water Lubricated Stainless Steels for a Spent Fuel Rack Facility," MIT, a report for Boston Edison Company, 1976.

22. Westinghouse Document No: APP-GW-G1-003, Rev. 3, "AP1000 Seismic Design Criteria," ~~Rev. 3,~~ May 2009. (Westinghouse Proprietary)

23. Deleted

24. LS-DYNA, v970 Livermore Software Technology Corporation, 2005.

~~25. RORARK'S Formulas for Stress & Strain, 6th edition, Warren C. Young, McGraw Hill.~~

25. Deleted

26. ASME Boiler & Pressure Vessel Code, Section III, Appendices, 1998 Edition with 2000 Addenda.

27. Westinghouse Calculation, APP-1230-CAC-001, Rev. 2, "Design of Spent Fuel Pit Floor in Module CA20," August 2008. (Westinghouse Proprietary)

28. U.S. NRC, Regulatory Guide 1.124, Rev. 1, "Service Limits and Loading Combinations for Class 1 Linear-Type Component Supports," January 1978.

29. Westinghouse Calculation: APP-GW-S2R-010, Rev. 3, "Extension of Nuclear Island Analysis to Soil Sites," November 2008. (Westinghouse Proprietary)

30. AP1000 Letter Number DCP/DCP1097, "Preliminary AP1000 Fuel Assembly Grid Impact Loads," from M. Misvel (Westinghouse Electric Company) to R. Morrow (Westinghouse Electric Company), Dated May 21, 2008. (Westinghouse Proprietary)

31. U.S. NRC Standard Review Plan NUREG-0800, SRP 3.8.4, Rev. 2, Appendix D, "Guidance on Spent Fuel Pool Racks," March 2007.

32. U.S. NRC, Regulatory Guide 1.124, Rev. 2, "Service Limits and Loading Combinations for Class 1 Linear-Type Component Supports," February 2007.

33. Westinghouse Calculation: APP-FS02-Z0C-001, Rev. 2, "Analyses of AP1000 Fuel Storage Racks Subjected to Fuel Drop Accidents," July 2009. (Westinghouse Proprietary)

~~1~~34. AP1000 Letter Number OBY_DCP_000469, "Impact Evaluation due to Spent Fuel Rack Reaction during a Seismic Event (Revise of OBY/DCP434)," Dated November 2, 2009. (Westinghouse Proprietary)

35. Westinghouse Calculation: APP-CA20-CAC-011, Rev. 1, "Auxiliary Building – CA20 Wall Basic Design Calculation," October 2007. (Westinghouse Proprietary)

36. Westinghouse Calculation: APP-1000-S2C-056, Rev. 1, "Nuclear Island Seismic Floor Response Spectra," October 2007. (Westinghouse Proprietary)

37. Westinghouse Calculation: APP-1000-S2C-093, Rev. 0, "Generation of Artificial Time History SSE Motion for Design of AP1000 Fuel Racks," May 2010. (Westinghouse Proprietary)

38. Westinghouse Calculation: APP-FS02-S3C-003, Rev. 1, "Artificial Time Histories for Westinghouse AP1000 Fuel Racks," September 2008. (Westinghouse Proprietary)

39. AP1000 Letter Number DCP_HII_000015, "Transmittal of Revised Fuel Rack Seismic Input per APP-1000-S2C-093", from S. M. Stipanovich (Westinghouse Electric Company) to Mr. Evan Rosenbaum (Holtec International), Dated May 26, 2010. (Westinghouse Proprietary)

40. Westinghouse Calculation: APP-1000-S2C-056, Rev. 2, "Nuclear Island Seismic Floor Response Spectra," March 2010. (Westinghouse Proprietary)

41. Westinghouse Calculation: APP-GW-S2R-010, Rev. 4, "Extension of Nuclear Island Analysis to Soil Sites," March 2010. (Westinghouse Proprietary)

42. Westinghouse Document: APP-FA01-V2-101, Rev. 2, "AP1000 Fuel Assembly Interface Parameters 17x17x168 Active Fuel (.374 DIA fuel Rod)," July 2009. (Westinghouse Proprietary)

43. Westinghouse Document: APP-FA01-V2-102, Rev. 2, "AP1000 Fuel Assembly 17x17x168 Active Fuel Sections and Details," July 2009. (Westinghouse Proprietary)

44. Westinghouse Calculation: APP-SFS-M3C-019, Rev. 1, "Calculation of Local Temperatures in AP1000 Spent Fuel Storage Racks," July 2008. (Westinghouse Proprietary)

~~5 DCD MARKUP~~

~~There are no DCD changes as a result of Revision 3 of APP-GW-GLR-033. All DCD markups were detailed in the RAIs that were the basis for this revision. The following RAI responses included a DCD markup:~~

- ~~RAI-SRP9.1.2-SEB1-04 (Revision 0) (which referred to RAI-SRP9.1.2-SEB1-01, Revision 0, for the actual DCD markups and was subsequently modified in RAI-SRP9.1.2-SEB1-01, Revision 1);~~

- ~~RAI-TR54-26 (Revision 1) (which was superseded by the DCD changes contained in RAI-SRP9.1.2-SEB1-06, Revision 1); and~~

- ~~RAI-SRP9.1.2-SEB1-06 (Revision 1) (which communicated an advance copy of changes that were made via DCP APP-GW-GEE-1185; the DCD will be changed using the DCP as the official basis).~~

~~The changes identified in those responses will be incorporated into a future revision of the DCD. Note that the spent fuel pool layout figure was slightly modified from the advance changes identified in the Revision 1 response to RAI-SRP9.1.2-SEB1-06; the corrected dimensions are shown in Figure 2-1 of this document, consistent with APP-GW-GEE-1185.~~